Development of Operational Guidelines for Recycled RO Membranes in UF Applications

Jawwad Ahmed

MSEE-00000277374

A thesis submitted in partial fulfillment of the requirements for the degree of

Master of Science

In

Environmental Engineering

Institute of Environmental Sciences and Engineering (IESE)

School of Civil and Environmental Engineering (SCEE)

National University of Sciences and Technology (NUST)

Islamabad, Pakistan

2020

Development of Operational Guidelines for Recycled RO Membranes in UF Applications

By

Jawwad Ahmed

00000277374

A thesis submitted in partial fulfillment of the requirements for the degree of

MASTER OF SCIENCE

In

ENVIRONMENTAL ENGINEERING

Institute of Environmental Sciences and Engineering (IESE)

School of Civil and Environmental Engineering (SCEE)

National University of Sciences and Technology (NUST)

Islamabad, Pakistan

2020

Certificate

It is certified that the contents and form of the thesis entitled **"Development of Operational Guidelines for Recycled RO Membranes in UF Applications"** submitted by **Mr. Jawwad Ahmed** has been found satisfactory for partial fulfillment of the requirements of the degree of Masters of Science in Environmental Engineering.

Supervisor: _____

Dr. Yousuf Jamal
Assistant Professor
IESE, SCEE, NUST

GEC Member: _____

Dr. Muhammad Taqi Mehran
Assistant Professor
SCME, NUST

GEC Member: _____

Dr. Muhammad Arshad
Associate Professor
IESE, SCEE, NUST

Thesis Acceptance Certificate

Certified that the final copy of MS thesis written by **Mr. Jawwad Ahmed**, Registration No. **00000277374** of **IESE (SCEE)** has been vetted by the undersigned, found complete in all respects as per NUST statutes/regulations, is free of plagiarism, errors, and mistakes and is accepted as partial fulfillment for award of MS degree. It is further certified that necessary amendments as pointed out by GEC members of the scholar have also been incorporated in the said thesis.

Supervisor: _____
Dr. Yousuf Jamal
Assistant Professor
(IESE, SCEE, NUST)

Head of Department: _____
Dr. Zeeshan Ali Khan
Assistant Professor
(IESE, SCEE, NUST)

Countersign by

Signature (Dean/Principal): _____
(SCEE, NUST)

Declaration

I certify that this research work titled **"Development of Operational Guidelines for Recycled RO Membranes in UF Applications"** is my own work. The work has not been presented elsewhere for assessment. The material that has been used from other sources has been properly acknowledged / referred.

Jawwad Ahmed
Reg # 00000277374

Acknowledgements

At the completion of my research study, first of all, I am exceptionally grateful to Almighty Allah for granting me the strength and capability accomplishing this task.

I am thankful to my family, in particular my parents, wife and daughters who stood by me throughout the duration of my course.

I am thankful to my employers, Prime Chemicals Corporation (Pvt) Ltd. and its directors, who allowed me to undertake this course while in their employment, and who also supported my research work by providing support in the form of equipment required for my experimental work for my thesis.

I also wish to document my gratitude to the organizers of the 1st International Conference on Water, Energy and Environment Nexus (WEEN-2019) held in Istanbul, for extending a discount worth USD 400 that allowed me to present my research at the conference, as well as editors of the journal Desalination and Water Treatment for waiving off the entire publication fee of up to EUR 180 in publishing our review paper.

I am also thankful to my supervisor Dr. Yousuf Jamal (IESE) and GEC members Dr. Taqi Mehran (SCME) and Dr. Muhammad Arshad (IESE) for their support, guidance and insightful criticism.

Jawwad Ahmed

Table of Contents

List of Figures

List of Tables

List of Abbreviations

AFM	Atomic Force Microscopy
ASTM	American Society for Testing and Materials
CAD	Computer Aided Design
CEB	Chemically Enhanced Backwash
CF	Cake Filtration
CFU	Colony Forming Unit
CIP	Clean In Place
COD	Chemical Oxygen Demand
CPB	Complete Pore Blocking
CTBD	Cooling Tower Blowdown
CW	Constructed Wetland
DOM	Dissolved Organic Matter
EAF	Electric Arc Furnace
EC	Electrical Conductivity
EPS	Extracellular Polymeric Substance
FTIR	Fourier Transform Infrared
GW	Grey Water
HEDP	1 Hydroxyethylidene 1,1 Diphosphonic Acid
HGW	High Strength Grey Water
HPMA	Hydrolyzed Polymaleic Anhydride
IESE	Institute of Environmental Sciences and Engineering
IPB	Intermediate Pore Blocking
LC-OCD	Liquid Chromatography – Organic Carbon Detection
LGW	Low Strength Grey Water
LMH	Liters per hour per square meter
MBR	Membrane Biofilm Reactor
MED	Multieffect Distillation
MF	Microfiltration
MFI	Modified Fouling Index
MPN	Most Probable Number
MSF	Multistage Flash Distillation
MWCO	Molecular Weight Cut Off
NF	Nanofiltration
NOM	Natural Organic Matter
NTU	Nephelometric Turbidity Units
PA	Polyamide
PAN	Polyacrylonitrile

PES	Polyether Sulfone
PSf	Poly Sulfone
PVDF	Polyvinylidene difluoride
PVP	Polyvinylpyrrolidone
RO	Reverse Osmosis
SDG	Sustainable Development Goals
SDI	Silt Density Index
SEM	Scanning Electron Microscope
SMP	Soluble Microbial Products
SOC	Synthetic Organic Carbon
SPB	Standard Pore Blocking
SWRO	Sea Water Reverse Osmosis
TFC	Thin Film Composite
TMP	Trans Membrane Pressure
UF	Ultrafiltration

Abstract

Reuse of discarded RO membranes as ultrafiltration membranes after recycling them through an oxidative process has been increasing over the years. While RO and ultrafiltration membrane manufacturers have well documented guidelines on operational parameters, there is little published work on development of operational guidelines for recycled RO membranes used in ultrafiltration applications especially with the realization that most commercially available RO membrane modules are of spiral wound construction, while those of ultrafiltration are mostly hollow-fiber. This work has attempted to develop a basic guideline to allow performance prediction of ultrafiltration modules recycled from discarded RO membranes through pilot testing in filtration applications of two low strength waste water streams. In terms of membrane performance, pilot testing with low strength grey water was able to demonstrate consistent filtrate turbidities of < 1 NTU and COD rejection of 70%. Pilot testing with cooling tower blowdown feed water further demonstrated filtrate SDI and MFI values < 1.0 and a minimum 3 log reduction in total coliform and E.coli. Membrane was able to operate at a flux range of 40 – 100 lmh with feed pressures of 2 – 4 bar. The results show that recycled discarded RO membranes have similar performance and operational characteristics as commercial ultrafiltration membranes.

Chapter 1: Introduction

1.1. Water Scarcity & the need for Desalination

Water scarcity is a recognized global issue. Over 500 million people have been reported to live in conditions of severe water scarcity for the whole of the year, while the number of people facing such conditions for at least one month of the year exceeds 4 billion (Mekonnen & Hoekstra, 2016). This is summarized in Figure 1, where water scarcity as a ratio of the fresh water footprint and availability is shown geographically for the whole world.

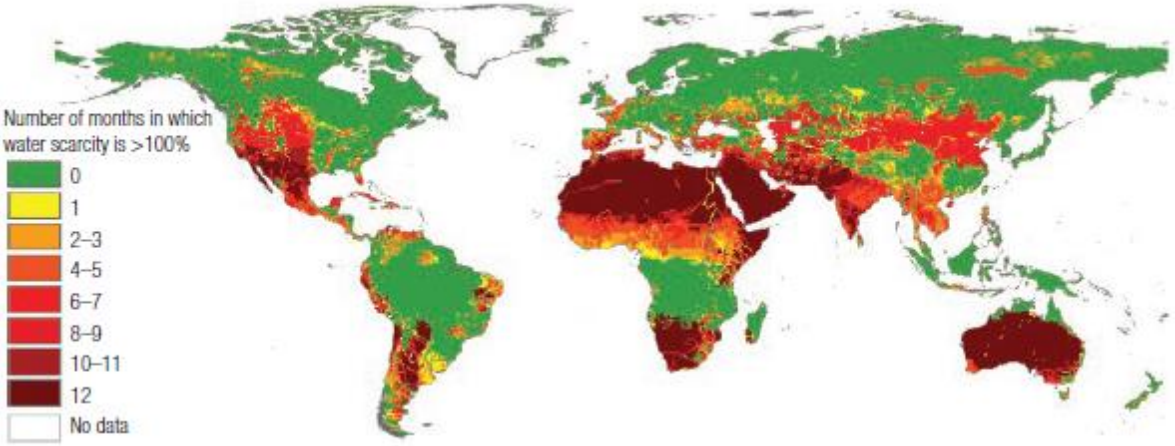

Figure 1: Regions that experience fresh water scarcity throughout the year for 1996-2005 (Mekonnen & Hoekstra, 2016)

Population growth and increased per capita water consumptions are expected to aggravate the stress on water scarcity, which is expected to be further exacerbated by the effects of climate change (Damania et al., 2017). These factors indicate how our conventional water sources may be insufficient to meet the increasing water demands, posing an obvious challenge to meeting the SDG (Sustainable Development Goal) 6.

Water scarcity, therefore, is fast becoming a major concern, and simultaneously, a driver for development of unconventional water resources. Some of the unconventional water augmentation that have been identified include fog harvesting, rain enhancement through cloud seeding, micro-catchment rainwater harvesting, deep onshore and offshore fresh-brackish groundwater, recycling of municipal wastewater, agricultural drainage water and desalination. Water recycling and reclamation activities as well as desalination for use of brackish and sea water are among the most

promising options in this regard with around 16,000 desalination plants currently operational worldwide producing over 95 million cubic meters of fresh water for potable use (Qadir, 2020).

1.2. Trends in Desalination & Reverse Osmosis (RO)

Desalination refers to the process of removing salts from water to allow it to meet the quality (salinity) requirements of different human uses (Darre & Toor, 2018). Historically, thermal desalination techniques, primarily Multistage Flash Distillation (MSF) and Multi-Effect Distillation (MED) were the technologies of choice for desalination plants. However, development of membrane technology has propelled Reverse Osmosis (RO) to be the technology of choice for desalination applications. This is shown in Figure 2, where the total desalination capacity and number of desalination plants is plotted against time on the primary axis, and the desalination capacity by technology is plotted in the inset against time, clearly indicated how RO has overtaken thermal desalination technologies in the 1990s, and constitutes the major share of the incremental desalination capacity in the last two decades (Jones et al., 2019).

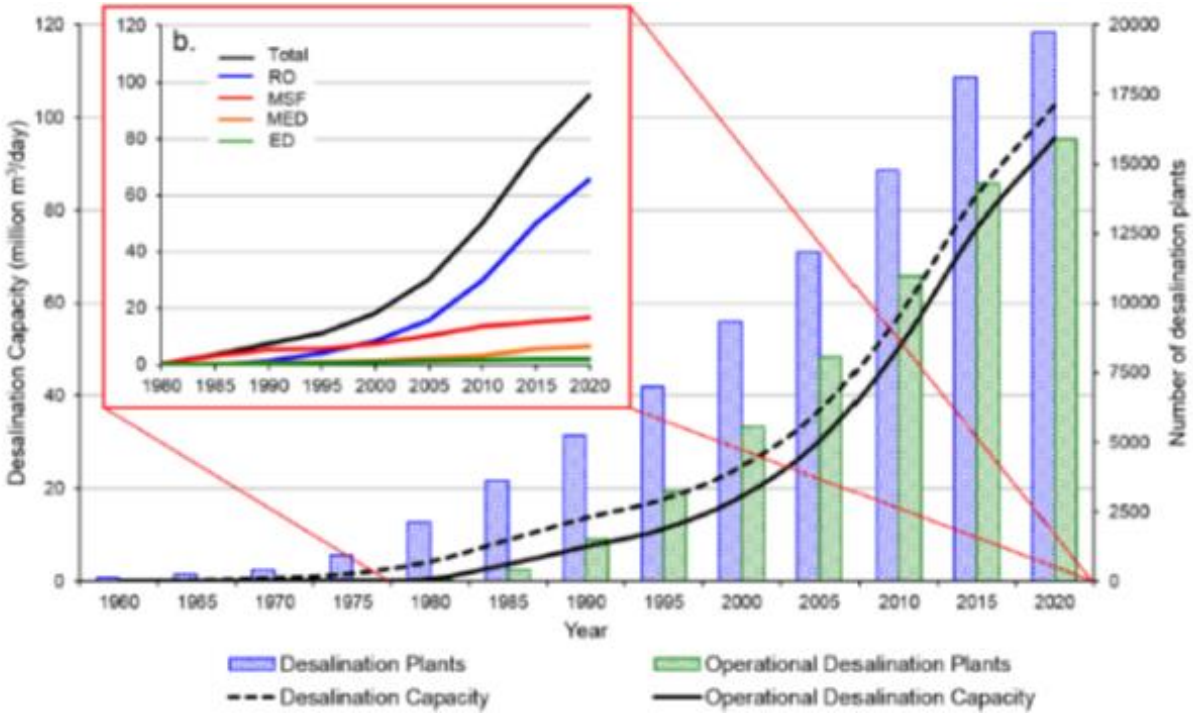

Figure 2: Trends in global desalination by desalination capacity and number of plants (Jones et al., 2019)

As is shown in Figure 2, Reverse Osmosis (RO) accounts for the major share of the global desalination market, with the thin film composite (TFC) membranes with polyamide as the active layer holding two-thirds of the share in terms of the total installed capacity (García-Pacheco et al., 2018; Virgili et al., 2016). After use in brackish and seawater desalination plants, over 840,000 end-of-life RO membranes are annually discarded, representing a solid waste generation of over 14,000 tonnes per annum worldwide (Landaburu-Aguirre et al., 2016).

Conventionally the discarded RO membranes are disposed of in landfills or incinerated, but recent studies have highlighted the potential of treating these used membranes for reuse in ultrafiltration (UF) applications. This potential is all the more appealing for developing countries, where membranes – both RO and UF – are exclusively imported.

1.3. Composition of conventional RO membranes

Most industrial and municipal RO plants today utilize either of the 4" or 8" diameter RO membranes, although the 16" diameter is also now being used for large scale Seawater RO (SWRO) desalination plants as well. Figure 3 shows a cut-away of an RO membrane module and its major parts. Table 1 lists the components of the RO membrane along with the material they are made of, and their relative weights. It can be seen that the active layer in RO membranes, the polyamide layer represents only 0.3% of the membrane weight. When this portion of the membrane is not able to perform its role, the entire membrane becomes useless and has to be discarded.

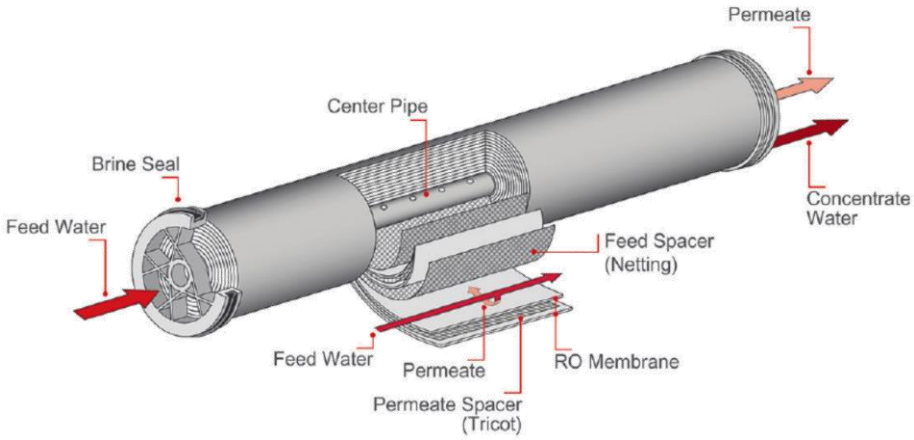

Figure 3: Components of conventional spiral wound RO membrane (Lanxess-Lewabrane, 2012)

Table 1: Composition of 8" Diameter RO Membrane (Hydranautics, 2018)

	Material	**Weight (Kg)**	**%age**
Outer Casing	Fiberglass	1.83	11.9%
Polyamide Active Layer	Polyamide	0.05	0.3%
Polysulfone Support Layer	Polysulfone	0.88	5.7%
Polyester Support Layer	Polyester	5.59	36.4%
Feed & Permeate Spacer	Polypropylene / Polyester	3.26	21.2%
Tube & End Caps	Acrylonitrite butadiene styrene	2.38	15.5%
Glued Parts	Polyurethane glue	1.37	8.9%

1.4. Disposal of RO membranes

Figure 4 shows the waste disposal hierarchy, which can also be applied to end-of-life RO membrane elements. The waste disposal hierarchy values waste reduction, reuse, recycling, energy recovery, treatment and disposal in decreasing order of preference. It is no surprise then, that current research in RO desalination is focused membrane fouling mitigation measures that aim to extend membrane life and therefore reduce waste, in addition to reducing capital and operational costs.

Direct membrane reuse – i.e. use of the membrane which has suffered from loss of operational flux, salt rejection or increase in differential pressure, after cleaning is common practice in the industry.

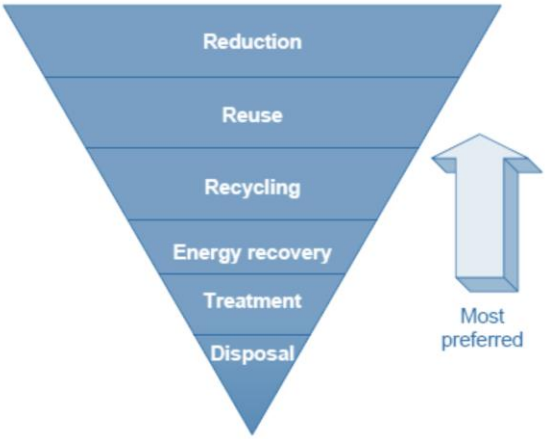

Figure 4: Waste Disposal Hierarchy

Although research has also focused on the remaining aspects of the disposal hierarchy with respect to discarded RO membranes, recycling RO membranes for use as ultrafiltration (UF) membranes is an exciting dimension, especially for developing countries that otherwise have to rely on imports for both RO and UF membranes.

The concept of membrane recycling realizes that the active layer in RO membranes is the polyamide layer, which is susceptible to degradation upon exposure to oxidants. Cross-section of the TFC membrane with active polyamide layer is shown in Figure 5. If this active layer is intentionally degraded to removal, it exposes the Polysulfone support layer which is 40-60 micrometers thick, but has a porosity range that qualifies it as an ultrafiltration membrane itself. By this in-situ chemical degradation, discarded RO membranes can be reconditioned into ultrafiltration membranes without having to dismantle the membrane at all. This is further discussed in detail in the subsequent chapters.

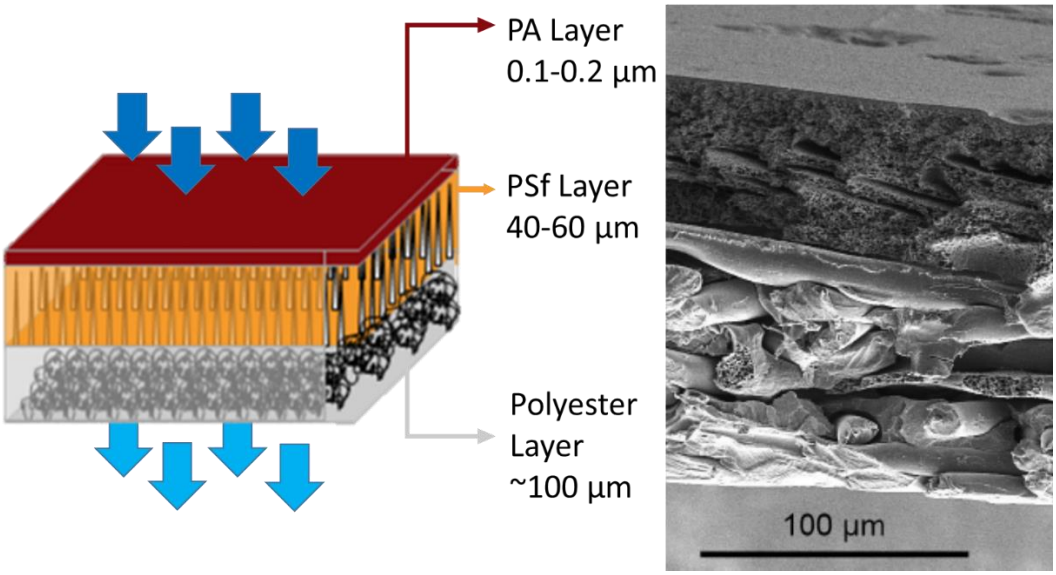

Figure 5: Cross section of a TFC RO Membrane

Chapter 2: Literature Review

2.1 RO Membrane Recycling

2.1.1. RO Membrane Active Layer Degradation

As discussed in the previous chapter, the concept of membrane recycling is borne out of the need to reduce solid waste generation, and the observation in the industry of the limited oxidant tolerance of the polyamide (PA) layer, which is the active layer in most commercial TFC RO membranes. RO membrane autopsy results have shown oxidation to be the second largest contributor to membrane failure after biofouling (Chesters et al., 2013). Because of the prevalent use of the chlorine as a disinfectant in upstream processes, it is the most important oxidant for studies on RO membrane degradation. Degradation of RO membranes through chlorine has extensively been studied. In this context, chlorine at low levels of exposure has been noted to impact the elasticity and permeability of the PA layer. At higher levels of exposure, chlorine leads to the formation of cracks and loss of material from the PA layer, which subsequently leads to a visible drop in membrane salt rejection (Gohil & Suresh, 2017; Shin et al., 2011; Verbeke et al., 2017).

The actual mechanism through which this degradation comes about has been discussed in literature. A closer look at the published literature reveals that multiple mechanisms through which oxidants degrade the PA layer have been studied. These include the following: (a) transformation of crystalline regions to an amorphous region due to disruption in the intermolecular hydrogen bonds and the symmetry of PA network, (b) delaminating of the PA skin layer, (c) increase in the hydrophobic nature of the PA layer, (d) substitution in the polyamide N-H link and/or the aromatic ring of chlorine atoms, (e) partial destruction of the rigid PA structure, leading to conformational changes, and an increased free volume and flexibility of the polymer chains, (f) tightening of the PA layer, and (g) formation of a soft barrier layer, which compacts under pressure and eventually collapses the polymer chains (Barassi & Borrmann, 2012; Kwon & Leckie, 2006a, 2006b). With regards to degradation of the PA layer in RO membranes, it has been argued that substitution in the polyamide N-H link and/or the aromatic ring of chlorine atoms (also known as Orton Rearrangement) is the most acceptable mechanism (Gohil & Suresh, 2017).

Halogenation reaction of the PA layer aromatic ring under normal conditions of RO membrane operation i.e. between 15 - 30˚C temperature is not thermodynamically favored. In the presence of a weak acid, however, the conditions start favoring ring chlorination (Solomons, 1997). Because chlorine, upon dissolution of water contributes, among other species, the hypochlorous acid, this provides the required condition of the presence of a weak acid that favors ring chlorination of the PA aromatic ring. This leads to degradation of the ring in the following ways: (a) Electrophilic substitution of chlorine atom on the aromatic ring, (b) Orton Rearrangement i.e. N-chloramine formation at the amide linkage after chlorine attack on the N-H bond. These reactions are shown in Figure 6.

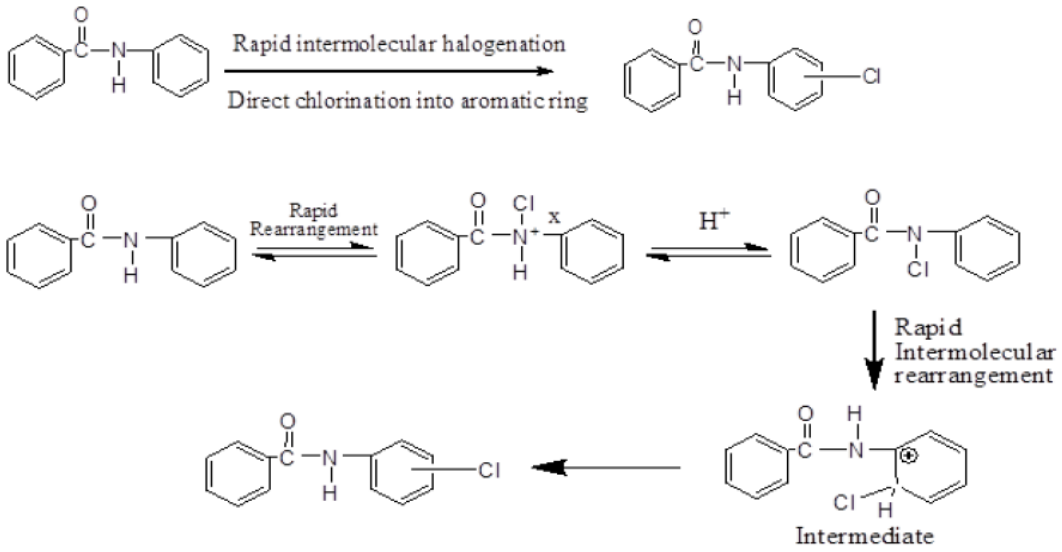

Figure 6: N-Halogenation and Orton Rearrangement reactions
(Gohil & Suresh, 2017)

Furthermore, the presence of transition metals like iron and aluminum during the process of oxidant degradation of the PA layer has also been shown in published literature to have a catalytic effect on the PA layer degradation (Tessaro et al., 2005).

Considering this degradation mechanism, the potential for recycling end-of-life RO membranes as ultrafiltration (UF) or microfiltration (MF) membranes has been identified by Rodriquez et al at least as early as 2002. They carried out testing on complete 8” diameter used sea water RO membrane elements by subjecting them to exposure with different oxidants, primarily potassium permanganate, to peel off the active polyamide layer from the RO membrane, and defined the

effectiveness of conversion from RO to UF/MF in terms of a 'peeling effectiveness', which was defined as a function of membrane product recovery, salt passage and the pressure required for the peeling off step (Rodríguez et al., 2002).

Veza and Rodriguez-Gonzalez put discarded end-of-life RO membranes after oxidative treatment with $KMnO_4$ in a pilot plant of around 6 m^3/hr flow and were able to reduce influent turbidities of 8 – 10 NTU to less than 0.1 NTU (> 90% reduction) with the recycled RO membrane preceded by a cartridge filter. The pilot plant application itself was a tertiary wastewater treatment application, and reported appreciable fouling for the recycled RO membrane elements (Veza & Rodriguez-Gonzalez, 2003). Although further studies noted limitation of $KMnO_4$ treatment in increasing the membrane permeability beyond a certain limit, it was found that this was due to deposition of manganese oxide layer on the membrane, which can be removed by treatment with citric acid (Ambrosi & Tessaro, 2013).

2.1.2. Membrane Conversion & Characterization

Prince et al. found sodium hypochlorite as an effective oxidant to convert RO membranes to UF ones, and found them to be comparable to "a regenerated cellulose UF membrane with molecular weight cut off of 10 kDa." While they found comparable hydraulic performance for both the recycled end-of-life RO membrane and a commercial UF membrane, they anticipated higher fouling potential for the reused RO membrane (Prince et al., 2011).

This has further been confirmed through experiments for membrane surface characterization, which have found higher surface roughness for converted RO membranes as compared to commercial UF membranes. Actual fouling experiments by Lawler et al. have also yielded similar results (Lawler, 2015).

In terms of oxidant effectiveness, hypochlorite has been found to be more effective for higher degradation intensities, allowing permeability of up to 170 Lmh/bar (against RO membrane permeability values of less than 5 Lmh/bar) using sodium hypochlorite solutions on the order of 300,000 ppm.h (Lawler et al., 2011; Pontié, 2015). Membrane permeability and salt rejection are

shown in Figure 7. Garcia-Pacheco et al. also claim guaranteed membrane conversion to ultrafiltration at 300,000 ppm.h NaOCl exposure (García-Pacheco et al., 2019).

SEM images (shown in Figure 8) of a treated RO membrane and a UF one also demonstrate similar profiles (Lawler et al., 2012). Input from FTIR spectroscopy has confirmed the mechanism of conversion to be the elimination of the polyamide layer as shown in Figure 9. Both these characterization experiments have separately been performed by Garcia-Pacheco et al. and have reported similar results (García-Pacheco et al., 2016).

Although UF membranes exhibit higher hydrophobicity, converted RO membranes have been shown to exhibit similar rejection properties of humic substances, biopolymers and low molecular weight building blocks, shown in Figure 10 through LC-OCD (Liquid Chromatograph-Organic Carbon Detection) profile of feed and filtrate water, as well as virus sized particles (Lawler et al., 2013; Raval et al., 2012), showing rejection characteristics comparable ultrafiltration membranes with a porosity between 10kDa and 30 kDa (Lawler, 2015), although Ravel et al. have reported a a value as high as 97 kDa (Raval et al., 2012).

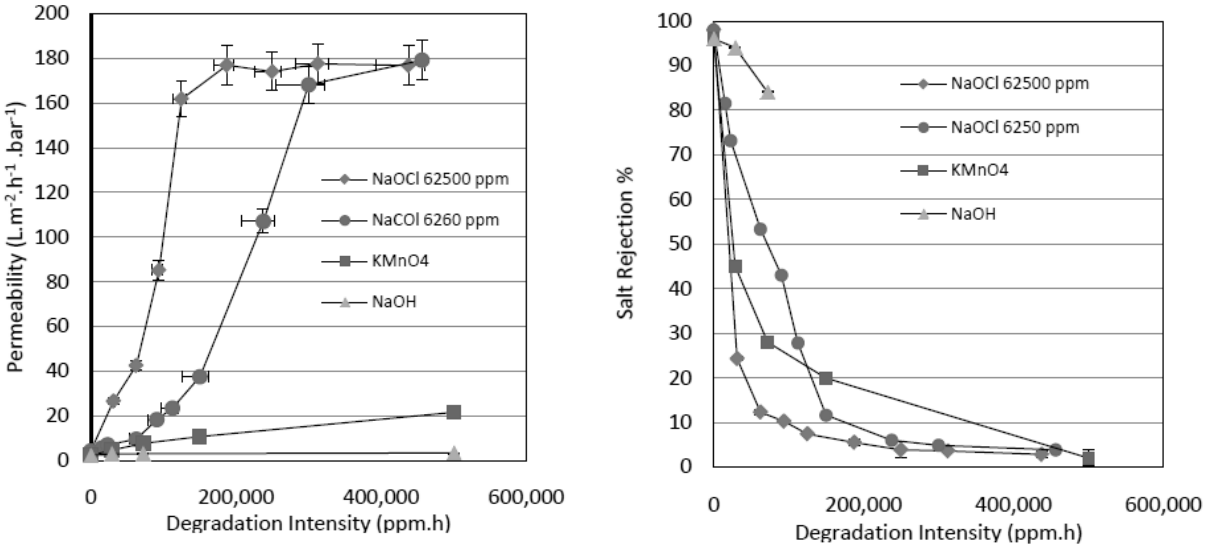

Figure 7: Membrane permeability & Salt Rejection vs degradation intensity (Lawler et al., 2011).

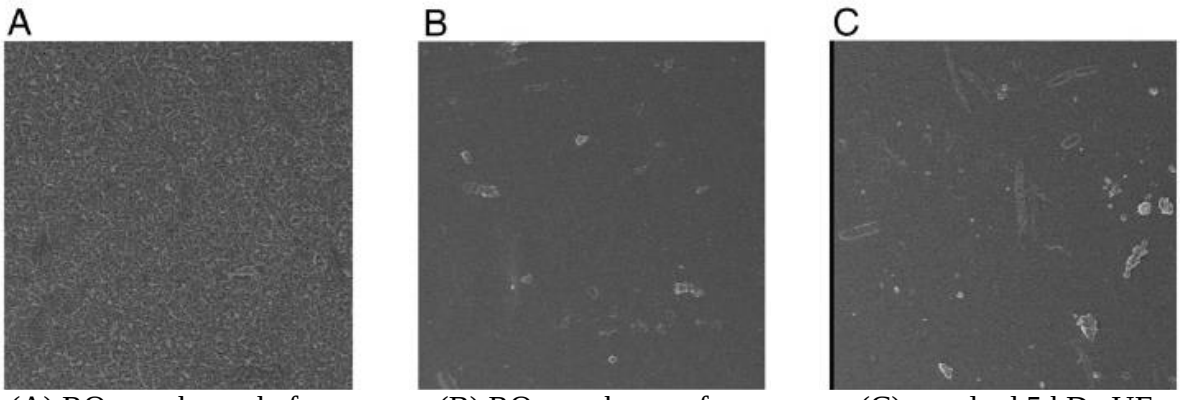

(A) RO membrane before conversion (B) RO membrane after conversion (C) standard 5 kDa UF membrane

Figure 8: SEM micrographs of membrane surface at 3,000 x magnification (Lawler et al., 2012).

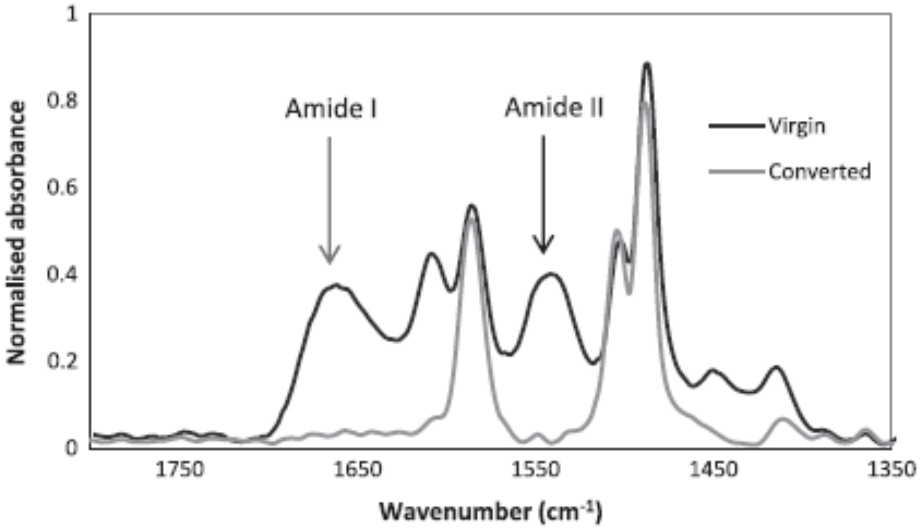

Figure 9: FTIR showing elimination of polyamide layer upon exposure to chlorine (Lawler et al., 2013).

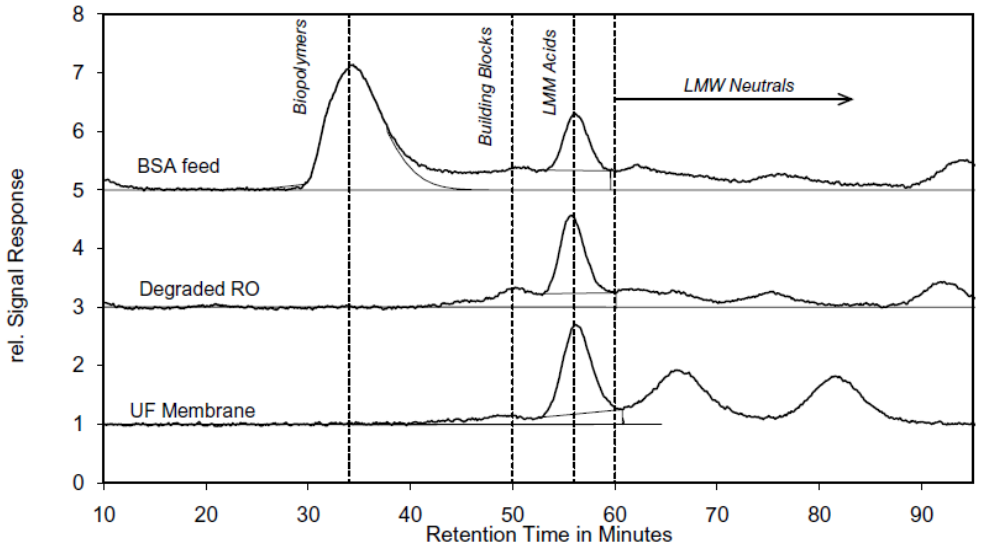

Figure 10: Feed and filtrate water LC-OCD profile of converted RO and 5 kDa UF membrane (Lawler et al., 2011).

The success of the process of conversion of RO membranes into UF ones, in addition to the oxidant dose, depends on the membrane storage, degree and pressure of pre-wetting, membrane application type (whether seawater or brackish water) and manufacturer (Lawler et al., 2013). Some of the pre-wetting options available include membrane pressurization, immersion in a 50% solution of ethanol-water or propanol-water for 15 mins, and immersion in 1% HCl or 4% HNO_3 for 1-100 hours (Coutinho de Paula & Amaral, 2017).

Furthermore, active degradation brought about by recirculation of the oxidant has been shown to bring about membrane degradation faster than passive degradation through soaking only (Antony et al., 2010). A recent study by Garcia-Pacheco et al. demonstrated a batch conversion process in which up to six RO membranes can be treated by varying hypochlorite exposure followed by sodium bisulfite exposure to reduce the residual chlorine at the end of the process (García-Pacheco et al., 2018).

Landaburu-Aguirre et al. have summarized the different studies for membrane conversion, characterization and operation, and noted that the converted membranes have been operated in both dead-end and cross-flow operational modes (Landaburu-Aguirre et al., 2016).

Polysulfone, which becomes the active layer upon the removal of the PA layer, has been covered extensively in published literature as a material for ultrafiltration membranes. It is noted to have performance competitive with other materials used in commercial ultrafiltration membranes. Other studies have specifically reported that, upon the degradation of the PA layer, the stability of the exposed underlying PSf layer of recycled RO membranes is not affected by further NaOCl exposure and has surface and solute rejection properties similar to those of commercial UF membranes (Molina et al., 2018).

2.1.3. Reuse as brackish water RO or Nanofiltration membranes

In other applications of recycling used RO membranes, Mohamedou et al. demonstrated that RO membranes lose permeability with age, and attain NF characteristics without the need for any treatment (Ould Mohamedou et al., 2010). Similar to the conversion process to ultrafiltration discussed earlier, it is expected that the automatic conversion to nanofiltration may also be inhibited by membrane condition, and oxidative treatment with sodium hypochlorite may be carried out – at limited concentrations – to accelerate the conversion (García-Pacheco et al., 2015; Moradi et al., 2019). Moreover, conversion of used sea water RO membranes through limited chlorine exposure to attain brackish water RO membrane characteristics has also been shown (García-Pacheco et al., 2018). Pontie et al. considered using discarded RO membranes for membrane distillation applications (Pontié et al., 2017).

2.1.4. Life Cycle Assessment of end-of-life RO membranes

Lawler et al. have further carried out a detailed comparative life cycle assessment of end-of-life options for RO membranes and concluded that recycling is the best alternative after for end-of-life RO membranes after direct reuse. Since the option of direct reuse is not available for a large fraction of the overall end-of-life RO membranes, recycling through conversion is the best available form of membrane disposal in terms of the relative impact on the environment (Lawler et al., 2015a; Lawler et al., 2015b). This is shown graphically in Figure 11, which compares the relative impacts on greenhouse gas emission and resource depletion of different disposal alternatives including direct disposal in landfill and incineration, energy recovery through

gasification and electric arc furnaces (EAF) and recycling membrane component material after shredding, in addition to the options of recycling for UF and direct reuse.

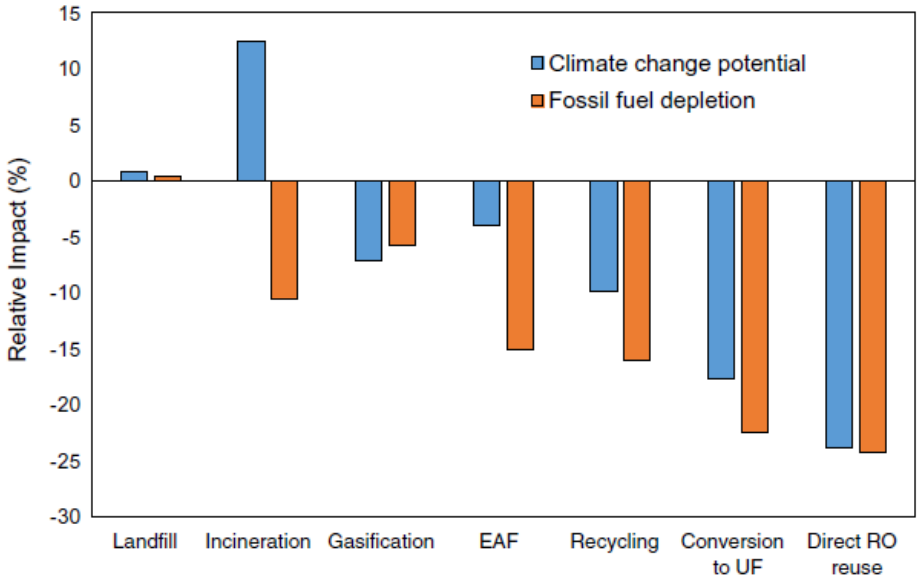

Figure 11: Greenhouse gas emissions and resource depletion for the disposal of RO membrane elements displayed as relative offset to membrane production.
(Lawler et al., 2015a)

Coutinho de Paula and Amaral have further estimated that using these recycled RO membranes in UF applications can allow monetary savings of almost 99% even if lower membrane life is considered for the recycled membranes, allowing not just an opportunity for reduction in solid waste but doing so in a sustainable way (Coutinho de Paula & Amaral, 2018). Other research groups have also estimated similar potential cost savings (Terrero et al., 2017).

2.2 Commercially Available UF and Converted Membrane Properties

2.2.1 Module Geometry and Operation Mode

Most commercially available RO membrane modules utilize spiral wound membranes, and are operated in cross-flow mode (Greenlee et al., 2009). Although 16" diameter modules have also been deployed in larger seawater desalination plants (Faigon, 2016), commonly used commercial modules are either 4" (with membrane surface area around 7 – 9 m^2) or 8" (with membrane surface area around 35 – 41 m^2) in diameter, and 40" in length across most manufacturers. Operational flux ranges across the membrane are typically specified by membrane manufacturers as a function

of the feed water source, and range from as low as around 10 lmh for seawaters to around 40 lmh for brackish waters with good pretreatment (Dow-Water-and-Process-Solutions, 2011b; Lanxess-Lewabrane, 2012).

In contrast to RO, most commercially available UF membranes utilize hollow-fiber membranes, and are mostly operated in dead-end mode. Moreover, and again in contrast to RO, most UF membranes are housed in manufacturer specific modules as part of proprietary systems such that many of the membrane properties specific to the manufacturer (Pilutti et al., 2003). Again, operational flux ranges across the membrane are typically specified by membrane manufacturers but are much higher than those for RO, ranging from around 40 lmh to 120 lmh, and sometimes even beyond (BASF-Inge, 2014; Dow-Water-and-Process-Solutions, 2011a). Important membrane characteristics of some hollow-fiber ultrafiltration membranes are shown in Table 2.

The feed water flow in spiral wound membranes is through what is called the feed spacer. The most common RO membrane models have a feed spacer thickness of 28-31 mils (0.7 – 0.8 mm), while 'fouling resistant' models have a feed spacer thickness of 34 mils (0.9 mm).

Table 2: Membrane Characteristics of some Hollow-Fiber Ultrafiltration membranes

Manufacturer	Models	Flow Direction	Pore Size (µm)	Material	Bore Dia (mm)	Chlorine tolerance (ppm / ppm.h)
Hydranautics	HYDRACap MAX 40, 60, 80	Outside-In	0.08	PVDF	0.60	5,000 / 750,000
DOW Dupont	SFP/D-2880, 2860, 2660	Outside-In	0.03	PVDF	0.70	2,000 / -
Microdyn-Nadir	UA1060	Outside-In	0.025	PAN	0.90	100 / 100,000
BASF inge	Dizzer 5000, etc	Inside-Out	0.02	PES	0.90	200 / 200,000
	Dizzer XL 1.5 MB, etc				1.50	
Norit X-Flow	Aquaflex 55	Inside-Out	0.02	PES/ PVP	0.80	200 / 250,000
	Aquaflex 64				0.83	

Hollow-fiber membranes come in two flow configurations. The inside-out models have feed water in the membrane bore flowing radially outwards as filtrate through the membrane. The outside-in models have feed water on the outside flowing radially into the membrane bore. For these models, the bore diameter is less important as the cleaner filtrate flows through the bore. For the inside-out

model, the bore size is more important as small bore sizes are more susceptible to fouling, and in general, only higher bores recommended for high feed water suspended solid loads.

While most UF membranes are in hollow-fiber construction, some manufacturers are also offering modules in spiral wound configurations. Secondly, while hollow-fiber operation is generally carried out in dead-end mode – cross-flow operation is considered unusual, although datasheets and product manuals of hollow fiber UF membranes sometime do suggest operation in a feed-and-bleed cross-flow mode for high fouling waters – the spiral wound UF membrane manufacturers exclusively suggest operation in cross-flow mode, the cross-flow velocity being generally a function of the feed spacer thickness. These are shown in Table 3.

Table 3: Membrane Characteristics of some Spiral Wound Ultrafiltration membranes

Manufacturer	Models	Suggested Cross-flow (m^3/hr)	Pore Size (μm)	Feed Spacer Thickness (mm)
Microdyn-Nadir	iSep 500 PES	-	0.03	2.3
Synder	MK (PES), ST (PES) 8" Dia	15	<0.01 (30 kDa)	0.61
		17		0.79
		20		1.17
	MK (PES), ST (PES) 4" Dia	3	<0.01 (30 kDa)	0.61
		4		0.79
		5		1.17
Alfa Laval	UF-PET/PHT/PP 8" Dia	18	<0.02 (100 kDa)	0.76
		29		1.22
		34		2.0
	UF-PET/PHT/PP 3.8" Dia	6	<0.02 (100 kDa)	0.76
		8		1.22
		11		2.0

It is noted that the makes provided in Table 3 are for generic ultrafiltration membranes, and not necessarily specific to the same for water treatment except for the Microdyn-Nadir, which is rated for high fouling waters with a suspended solids concentration of 1,000 mg/L. The model allows for single membrane modules connected in parallel with the driving force for filtration actually coming from the filtrate side through the suction generated by the product pump.

2.2.2 Membrane Porosity

Commercially available UF membranes comes in a variety of pore sizes, but it has been observed that a single pore size is generally specific to the manufacturer. Important membrane characteristics of different hollow-fiber UF membrane manufacturers are tabulated in table 1. AFM (Atomic Force Microscopy) is one of the techniques used to characterize membrane pore sizes, and although uncertainties still exist in developing correlation among AFM measurements and MWCO, the corresponding pore size of the converted RO membranes is likely to be < 0.01 μm based on published attempts at the correlation from literature (Bowen & Doneva, 2000; Dietz et al., 1992; Ren et al., 2006).

2.2.3 Membrane Materials

Membrane materials of different manufacturers are also provided in table 1. The membrane materials, in addition to the selectivity for suspended solids given through the MWCO or the pore size, are generally characterized by a reasonably good tolerance to exposure to acid, bases and oxidants. While the polyamide layer of the RO membranes have very poor tolerance to oxidants, peeling off this layer – as described in preceding section(s) – exposes the polysulfone (PSf) layer, which is otherwise the support layer for RO operation, but will become the active filtration layer for the converted membrane operation. PSf as a material for ultrafiltration membranes is well studied (Mulder, 2012).

UF membranes are also characterized by their chlorine tolerance, as chlorine, primarily in the form of sodium hypochlorite, is used for cleaning of the membranes of organics and biological growth. As shown in Table 1, PVDF membranes are rated for a higher chlorine tolerance than PAN and PES membranes. In fact, comparison among the PVDF and Polysulfone membranes have shown much higher chlorine resistance for PVDF as compared to PSf, with the PSf membranes susceptible to pore swelling and decreased rejection of characterizing substances with increasing chlorine exposure (Zhang et al., 2017). Realizing that Hypochlorous acid is the form of chlorine that is actually responsible for the degradation of membranes, it is understandable that the chlorine exposure values in Table 1 are qualified in membrane datasheets with a pH of 10 and above, whence hypochlorite is the dominant chlorine form. In any case, the mechanism for membrane

degradation has been proposed as chain scission leading to mechanical weakening and polymer (PSf) relaxation (Causserand et al., 2008; Rouaix et al., 2006).

In comparison to other materials, PSf membranes are known to exhibit better chlorine resistance than PAN and comparable to PES. PSf membranes are also known to exhibit a greater tolerance to different pH conditions than PVDF, PAN and PES material. PSf membranes are also tolerant to temperatures as high as 75°C (Shi et al., 2014).

2.2.4 Membrane wettability

Martínez et al. investigated additionally the wettability of the converted membranes through measurement of the contact angle. They found the converted RO membranes to have a contact angle between 60˚ and 80˚, suggesting a generally hydrophobic character of the converted membranes. They observed that membranes with inorganic fouling prior to being discarded had lower contact angles than membranes with organic fouling i.e. membranes with inorganic fouling had lower hydrophobicity than membranes with organic fouling (Martínez et al., 2015). These results are similar to those report elsewhere with a comparison of a contact angle of 70˚ for a converted RO membrane against that of 83˚ for a 10 kDa commercial UF membrane (Lawler et al., 2013).

2.3 Membrane Fouling & Feed Water Limitations

2.3.1 Converted Membrane Fouling

Membrane fouling is recognized as one of the most important problems for membrane systems. Fouling of the membrane entails shorter membrane life, increased operational costs, additional maintenance and chemical cleaning costs, and requires effective techniques for its mitigation. Different anti-fouling mechanisms have been covered in published literature. These deal with one of the two forms of anti-fouling measures: (i) preventive measures, which aim to reduce or eliminate the advent of fouling altogether, and (ii) recovery measures, which aim to recover the loss in performance due to fouling through cleaning measures (Shi et al., 2014).

2.3.2 Forms of Fouling

Fouling in ultrafiltration membranes takes place through multiple mechanics that include adsorption, pore blocking and cake formation.

Membrane fouling through adsorption takes place through interaction among the solutes or particles in the feed water with the membrane. Depending on the functional groups involved, these interactions can be due to van der Waals forces, electrostatic attraction or chemical bonding (Shi et al., 2014). Membrane fouling through pore blockage takes place due to the full or partial blockage of the membrane pores by colloids and particles. The onset of pore blockage usually occurs during the initial stages of filtration when the influent particles in the feed water directly come into contact with the membrane surface and pores (Field & Wu, 2011). Membrane fouling through cake (or gel) formation occur through the build-up of layers of particles on the membrane surface. The cake layers can itself be made up of particulates, colloids, organics or even a bio-organics.

Whatever the mechanism, in terms of the holistic composition of the foulants, these are generally categorized among particulates, organics, inorganics and biological foulants. Particulates (and colloids) can be organic or inorganic and physically block the membrane surface and its pores, leading to the formation of a cake layer on the membrane surface. Organics included dissolved components and colloids, such as Natural Organic Matter (NOM) in the form of humic acids,

fulvic acids, proteins, etc) which can attach onto the membrane through adsorption. Inorganic foulants refer to those in dissolved form which tend to precipitate, as a result of a chemical reaction like oxidation or solubility limits, onto the membrane surface. Biological foulants includes micro-biological organisms that can adhere to the membrane surface and develop a biofilm layer by secreting Extracellular Polymeric Substances (EPS) which provides additional adhesive properties on the cake layer (Guo et al., 2012).

Particulates and colloids have been differentiated in that colloids refer to suspended particles less than 1 μm in size, while particulates are generally referred to as those above this size. The mechanisms of particulate / colloidal fouling include pore blocking and cake formation. Pore blocking represents the onset of particulate fouling. Subsequently, as additional particles continue to deposit on the initial layer, a cake layer develops. When this happens, the cake layer starts to control transport and removal (Pearce, 2007).

Organics, both in dissolved and suspended form can also foul ultrafiltration membranes. Dissolved Organic Matter (DOM) is present in most natural waters, especially surface water sources. The organic matter can further be in the form of NOM, synthetic organic compounds (SOC) or soluble microbial products (SMP) formed during the biological treatment process in wastewater treatment plants. NOM is the most prevalent and important part of the overall organics, and is made up of different compounds formed as a result of decomposition of larger living organisms. This complex can be further considered to be composed of humic and fulvic acids, amino acids, proteins and carbohydrates. NOM may foul membrane through direct adsorption on the membrane surface, blocking access to pores and forming a gel layer (Guo et al., 2012).

While scaling and fouling through inorganics is more of a problem in RO and NF applications, under certain circumstances, it may be incident in UF applications as well. Thermodynamically, onset of scaling can only occur when the solubility of the respective cations and anions in the water are already beyond the solubility limit. However, as coagulants are often used in membrane treatment processes, they can themselves cause fouling on the membrane, as reported for iron based coagulants (Scott, 1995).

Biofouling is known to be one of the most serious forms of membrane fouling. Onset of biofouling takes places by deposition of microorganism on the membrane surface, followed by their growth and metabolism thereon. This results in the formation of a biofilm on the membrane surface, and can be described in the following steps: (i) attachment of planktonic bacteria onto the membrane surface, (ii) formation of colonies, (iii) development of mature biofilms. When the biofilm develops, it is dominated with EPS, cell debris of dead cells in addition to the living microorganisms (Guo et al., 2012).

2.3.3 Fouling Models

Because fouling leads to increased resistance to flow of water, this either results in an increase in the TMP or a decrease in flux. Hermia described four hypothetical fouling mechanisms for porous membranes, which continue to be referred in most modern work even today. These include: (i) complete pore blocking (CPB); (ii) standard blocking model (SBM); (iii) partial or intermediate pore blocking (IPB); and (iv) cake filtration (CF) (Hermia, 1982).

CPB model assumes that the particles are incident on the membrane and seal its pores such that they are not superimposed on each other. The blocked surface area is, then, directly proportional to the filtrate volume. SBM model assumes that the particle diameter is much less than the membrane's pore diameters, such that the particles enter the pore and deposit on the pore walls, reducing the pore volume. In this case, the decrease in pore volume is proportional to the filtrate volume. IPB model is similar to the CPB model except that in this case, there is provision of particles' superimposition on each other. The CF model is used to explain flux decline (or pressure increase) due to the formation of a cake layer (Mohammadi et al., 2003). These models are graphically shown in Figure 12.

These models have been adapted both for the constant pressure condition and the constant flux condition. Equations for the constant pressure condition, which is generally kept for pilot applications, are presented in Table 4 from the following general equation (Salahi et al., 2010):

$$\frac{d^2t}{dV^2} = K\left(\frac{dt}{dV}\right)^n$$

where the parameter n takes the value of 2 for CPB, 3/2 for SPB, 1 for IPB and 0 for CF model .

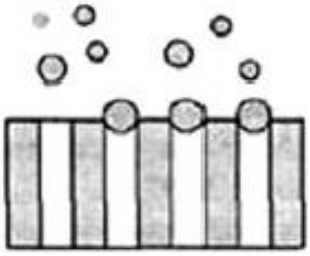

(a) Complete Bore Blocking model

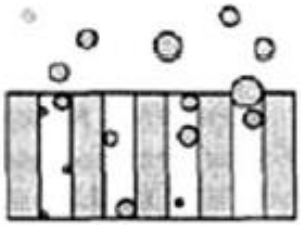

(b) Standard Blocking model

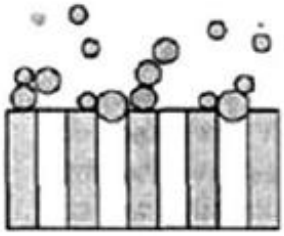

(c) Intermediate Pore Blocking Model

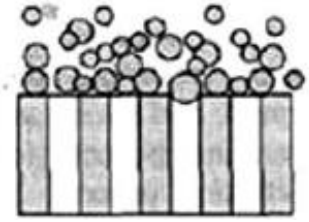

(d) Cake Filtration model

Figure 12: Graphical Representation of Blocking Models
(Salahi et al., 2010)

Table 4: Constant Pressure Fouling Model Equations (Salahi et al., 2010)

Model Name	**Model Equation**	**Linearized Form of Equation**
Complete Bore Blocking model	$J = J_0 e^{-K_c t}$	$\ln J = \ln J_0 + K_c\, t$
Standard Blocking model	$J = \frac{J_0}{(1 + K_s t)^2}$	$\frac{1}{J^{\frac{1}{2}}} = \frac{1}{J_0^{\frac{1}{2}}} + K_s\, t$
Intermediate Pore Blocking Model	$J = \frac{J_0}{1 + K_i t}$	$\frac{1}{J} = \frac{1}{J_0} + K_i\, t$
Cake Filtration model	$J = \frac{J_0}{\sqrt{1 + K_{gl} t}}$	$\frac{1}{J^2} = \frac{1}{J_0^2} + K_{gl}\, t$

Furthermore, the following equations further help to explain the models:

$K_c = K_A J_0$

$K_i = K_A$

$K_s = 2\frac{K_B}{A_0}\, A\sqrt{J_0}$

$K_{gl} = \frac{2R_g K_D}{J_0 R_m}$

Where:

J filtrate flux in $m^3/m^2/s$

J_0 initial filtrate flux in $m^3/m^2/s$

t time in s

K constant in general equation (units depend on fouling method; see below)

n constant in general equation

V accumulated filtrate volume in m^3

K_A constant used in CPB and IPB representing membrane surface blocked per unit of total volume filtered through the membrane in m^{-1}

K_B constant used in SPB representing the decrease in the cross-sectional area of the membrane pores per unit of total volume filtered through the membrane in m^{-1}

K_c constant used in CPB in s^{-1}

K_D constant used in CF representing the cake layer area per unit of total volume filtered through the membrane in m^{-1}

K_{gl} constant used in CF in s/m^2

K_i constant used in IPB in m^{-1}

K_s constant used in SPB in m^{-1}

A membrane surface area in m^2

A_0 membrane porous surface area in m^2

2.3.4 Anti-fouling Measures

Many anti-fouling methods have been described in literature. Practical applicability, however, limits these to the following for most ultrafiltration applications (Pearce, 2007):

a) Backwash

   Backwash entails flow in the opposite direction to the flow in service mode, which allows reversal of the effect of pore clogging and subsequent removal of the particulates from the membrane surface.

b) Air scour

Use of air scouring is carried out to induce shear forces, and thereby remove the foulants from the membrane surface. It is known to be effective for reverse pore clogging, and can significantly reduce requirements for chemical cleaning (Hilal et al., 2005).

c) Forward flush

Forward flush can be carried out to remove build-up of particle concentration on the membrane surface through the effect of shearing.

d) Chemically Enhanced Backwash (CEB)

CEB is similar to backwash, except that cleaning chemicals are used with the backwash water to combat specific types of foulants. For example, alkaline chemicals and/or oxidants are often used to remove organic foulants, and acidic chemicals are used to combat inorganic foulants.

e) Clean-in-Place (CIP)

CIP also used chemicals to remove the foulants except that a circulation loop is provided as part of the system, and cleaning takes place with the effect of chemicals within this loop, after which the chemical solution is discarded. The chemicals used in CIP are similar to those for CEB.

f) Other Measures

Many other approaches have been discussed in published literature, but are either variants of those described above or often not practical for commercial implementation. One measure that is often recommended is the introduction of a cross-flow velocity that help provide shearing forces during operation preventing deposition of the particles and further allowing them to be continuously flushed out of the system.

2.3.5 Feed Water Pretreatment for Fouling Control

This approach is extensively used to remove a portion of primarily particulates to mitigate membrane fouling by these particulates. Physical processes are commonly applied, and include

prefiltration and sedimentation. Coagulants and flocculants may further be used to enhance the effect of the pretreatment (Hilal et al., 2005). Most ultrafiltration membrane manufacturers stipulate a prefilter in the range of 100 – 500 microns upstream of ultrafiltration membranes (Crittenden et al., 2012).

2.4 Areas of Potential Applications of Converted RO Membranes

Potential areas of application of converted RO membranes are essentially same as those for which conventional ultrafiltration has been considered. Additionally, the life cycle costs of the converted RO membranes are expected to be much lower than that for conventional ultrafiltration membranes. García-Pacheco et al. have additionally considered the importance of recycling of RO membranes as part of a circular economy, and the need to project use of recycled membranes as an eco-innovation. Among the recognized areas of application are: tertiary wastewater recycling especially in decentralized treatment facilities, industrial wastewater recycling applications, including treatment of wastewater from landfill leachates, animal husbandries, textile, pharmaceutical or food industries and low-cost membrane solutions for drinking water treatment (García-Pacheco et al., 2017).

Recycled membranes are now also being considered for membrane biofilm reactor (MBR) applications, which is a form of ultrafiltration using submerged membranes for secondary effluent filtration (Morón-López & Molina, 2020; Morón-López et al., 2019).

In addition to the above, the following other direction applications are identified:

- Recycling cooling tower blowdown (CTBD) water
- Recycling low strength grey water (LGW)

Literature review of ultrafiltration to recycle these streams is discussed in the following sections.

2.5 Cooling Tower Blowdown (CTBD) Water Recycling

Cooling tower is an equipment extensively used in industry to reject waste heat from different process systems to the atmosphere through evaporation of water and subsequent cooling of this cooling water to a lower temperature. As heat rejection is through evaporation – and realizing that during the evaporation of water, the suspended and dissolved solids present in the water are retained in the system – the remaining cooling water is concentrated in concentrations of dissolved and suspended solids. A portion of the remaining water is bled off from the system so that the phenomenon of concentration does not go on indefinitely.

The bleed off is controlled to maintain a target cycle of concertation in the cooling water system, which is in turn limited by water chemistry and chemical additives for corrosion and scale inhibition. The bleed-off water is also referred to as blow-down, and is regarded as a waste stream from industry. CTBD streams represent a significant portion of the overall wastewater generated (van Limpt & van der Wal, 2014).

Recycling of CTBD water streams have been studied in published literature by different techniques and unit processes, including:

(a) coagulation-filtration followed by RO (Frick et al., 2014)
(b) membrane distillation (Ma et al., 2018)
(c) constructed wetlands (CW) followed by membrane treatment scheme (Wagner et al., 2018)
(d) nanofiltration (Zhang et al., 2020)
(e) ultrafiltration / microfiltration followed by RO (Farahani et al., 2016)

Ahmed et al. reviewed these technologies and found that ultrafiltration has been the technology of choice for CTBD recycling in most full scale applications. They concluded that the primary challenge in recycling CTBD is desalination through RO, but owing to the challenging nature of the CTBD water including those of organics, particulates and chemicals used for corrosion, scale and biological control, use of membrane prefiltration in the form of either ultrafiltration or microfiltration is necessary for most cases. They have identified potential for particulates characterized by turbidity, and organics characterized by either TOC (total organic carbon) or COD (chemical oxygen demand) among the major primary foulants. They have also identified the

potential role of sparsely soluble anions and cations in the water to cause scaling due to the concentration effect in the cooling tower. Furthermore, chemicals used in the cooling tower such as phosphates have a role in accelerating biofouling in the membranes by providing nutrients for uptake for the microbial consortia in the blowdown water. Table 5 shows a summary of the CTBD water parameters reported in published literature along with, where applicable, limits for feed water for RO – that is, those required for the filtration of the ultrafiltration system – as covered in published literature (Ahmed et al., 2020).

Table 5: CTBD water quality parameters and limits for RO feed water in literature (Ahmed et al., 2020).

Parameter	Units	Range from past literature on CTBD	Potential effect on RO membrane
pH		6.7 – 9.2	The effect of individual chemical constituents (anions and cations) depends on the relative abundance and conditions (pH, temperature) for favoring scale formation through precipitation upon exceeding the solubility limits in water. At moderate recoveries, calcium carbonate scaling is a concern. At higher recoveries, calcium sulfate, magnesium sulfate, calcium phosphate, barium and strontium sulfate and silicate scaling are also expected to be a concern.
Conductivity	µS/cm	1,500 – 7,132	
M-Alkalinity	mg/L as $CaCO_3$	54 – 356	
Sulfate	mg/L	407 – 2,341	
Chloride	mg/L	336 – 766	
Phosphate	mg/L	0.9 – 8.2	
Nitrate	mg/L	19 – 88	
Silica	mg/L	0.9 – 140	
Calcium	mg/L as $CaCO_3$	455 – 1,204	
Magnesium	mg/L as $CaCO_3$	43 – 470	
Sodium	mg/L	332 – 1,158	
Potassium	mg/L	52 – 81	
Barium	mg/L	0.145	
Strontium	mg/L	1.2 – 1.5	
TSS	mg/L	10 – 32	Accelerated fouling if > 1.0 mg/L
Turbidity	NTU	7 – 74	Accelerated fouling if > 0.1 NTU
TDS	mg/L	893 – 4,749	
TOC	mg/L	2 – 60	Accelerated fouling if > 2.0 mg/L
COD	mg/L	3.5 – 181	Accelerated fouling if > 10.0 mg/L

It can be seen from Table 5 that particulates and organics are the two major classes of contaminants that a UF membrane system must address upstream of RO membranes to limit fouling therein.

2.6 Low Strength Grey Water (LGW) Recycling

Grey water (GW) refers to household wastewater generated from kitchen sinks, bathroom sinks, showers and/or baths, and laundries, but excludes sewage generated from toilet flush water (Saumya et al., 2015). Grey water has been classified in published literature as being either low pollutant load (or low strength) GW (LGW) or high pollutant load (or high strength) GW (HGW), with the latter including waste streams from laundry and kitchen in addition to the LGW streams from showers and washrooms (handwashing and ablution) (Boyjoo et al., 2013).

The volume and pattern of greywater generated in a household is variable and is influenced by the total water consumption, water supply, number & age distribution of household members and lifestyles. Different studies have covered grey water reclamation through recycling and reuse using conventional physico-chemical and membrane based treatment process. In general, it has been described as an easy to treat alternative source of urban clean water as grey water has low concentrations of organic pollutants and pathogens (Revitt et al., 2011).

Li et al. have reviewed the different technologies used for grey water treatment for recycling, and summarized the available options (Li et al., 2009). These are presented in Figure 13.

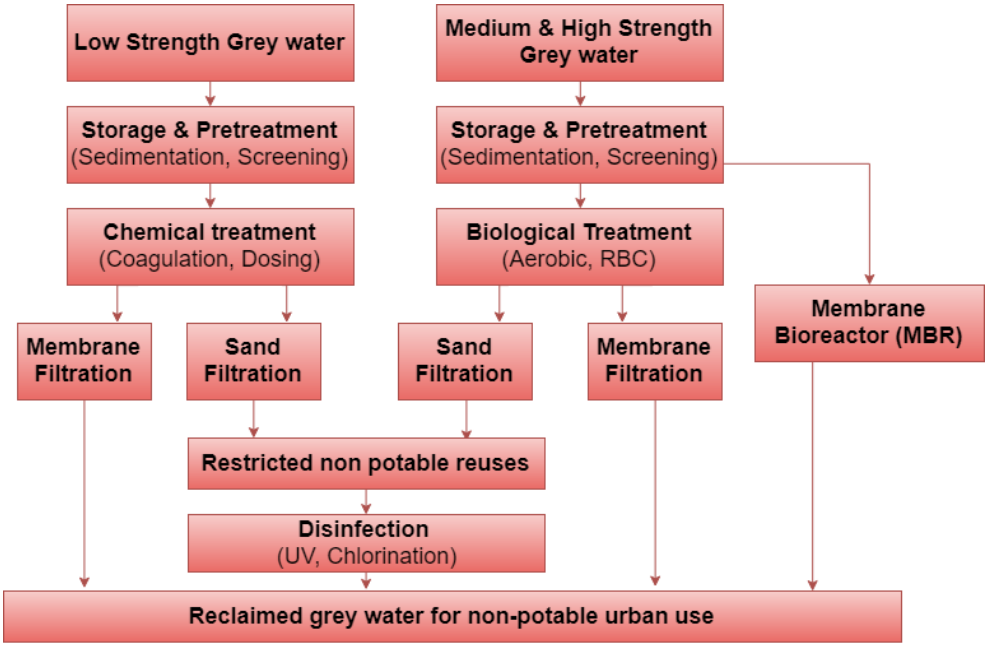

Figure 13: Grey Water Treatment Technologies
(Li et al., 2009)

Chapter 3: Materials & Methods

3.1. Removal of Active Polyamide Layer

3.1.1. Discarded RO Membranes

Discarded 4" diameter brackish water RO membranes from DOW Filmtec (BW30-4040) and Lanxess Lewabrane (B085 HF 4040) were used in this study. The membranes have an active membrane area of 7.2 m^2 and 7.9 m^2 and a feed spacer thickness of 0.86 mm and 0.79 mm respectively. Both membranes had formerly been deployed in Karachi, Pakistan to treat brackish water from underground wells and municipal supply. The Filmtec membrane had been discarded after 18 months of use, while the Lanxess Lewabrane membrane had been discarded after 12 month of use, after heavy particulate fouling when operators bypassed upstream safety measures, which allowed residual silt from feed tanks' bottom to pass on to the membranes.

Both membranes were separately deployed in single-stage single-element membrane vessels with an operational permeate flux of 25.0 lmh at a feed pressure of 12 bar. The operational membrane permeability, therefore, is calculated to be 2.1 lmh/bar. The pretreatment for both membrane systems was included dual stage multimedia filtration using silica sand and gravel in the first and Granular Activated Carbon adsorption in the second stage. This was followed by 5 microns porosity cartridge filters. The membranes has to be discarded after a rapid fall in the permeate flux to less than 10 lmh for both membranes, corresponding to a permeability of 0.83 lmh/bar, while salt rejection was greater than 95% for both membranes.

3.1.2. Membrane Cleaning

The discarded membranes were cleaned in steps of alkaline and acidic cleaning. The cleaning procedure adopted was largely as per the cleaning procedure provided by the membrane manufacturers. Alkaline cleaning was performed through recirculation in a solution of 0.1% sodium hydroxide (NaOH) and 0.025% surfactant (Sodium Dodecyl Sulfate) at a pH of 11.8 for over 2 hours, followed by a soak time of over 10 hours, after which the system was flushed. Acidic cleaning was performed through recirculation of solution of 0.2% hydrochloric acid at a pH of 1-2 for 2 hours.

3.1.3. Membrane Conversion

The cleaned membranes were subjected to exposure to a solution of 6.0% sodium hypochlorite (NaOCl) for 5 hours. This corresponded to an exposure of 60,000 ppm x 5h = 300,000 ppm.h. Industrial grade chemicals were used for cleaning and conversion to simulate conditions for commercial conversion of end-of-life RO membranes for recycling.

The schematic diagram of the equipment and setup used for membrane cleaning and conversion processes is shown in Figure 14. CAD model and picture of the apparatus are shown in Figure 15.

Salt rejection of the converted membranes was assessed by comparing the feed water conductivity with permeate water conductivity. Electrical Conductivity for salt rejection tests was measured using benchtop conductivity meter.

3.2. Feed Water

3.2.1. Grey Water

The apparatus outlined in the previous section for the membrane cleaning and conversion processes was thereafter used for performance and fouling tests for the converted membrane.

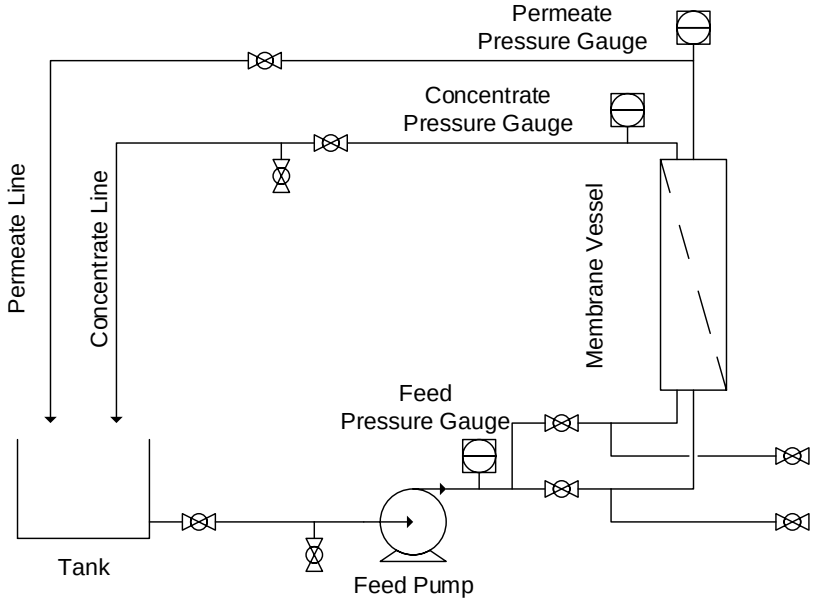

Figure 14: Schematic Diagram of membrane cleaning and conversion apparatus.

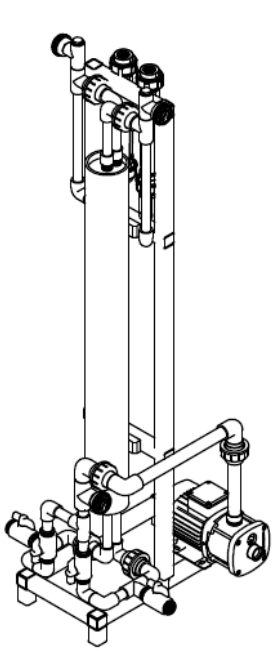

(a) CAD Diagram of apparatus

(b) Picture of apparatus

Figure 15: CAD Diagram and picture of cleaning, conversion and testing apparatus.

Grey water used for this study was low-strength grey water taken from a drain in a bathroom at IESE (Institute of Environmental Sciences & Engineering), consisting of wastewater from hand washing, ablution and floor cleaning activities. Comparison of the waste water parameters to those in literature further confirmed that the grey water used for this study was indeed low strength. The parameters are shown in Table 6. Diurnal grey water generation profile is shown in figure 16.

Table 6: Grey Water parameters used in current and past studies.

	Current Study	**Grey Water in literature (Boyjoo et al., 2013)**	**Low Strength Grey Water in literature (Boyjoo et al., 2013)**
Water Source	Bathroom + Ablution + Floor Cleaning	LGW + Kitchen + Laundry	Bathroom + Ablution + Cleaning
pH	7.6 – 7.9	6.3 – 10	
Conductivity (µS/cm)	1,000 - 1,100	80 – 1,800	
Turbidity (NTU)	24	20 – 440	12 – 375
COD (mg/L)	99	< 3,000	50 – 600

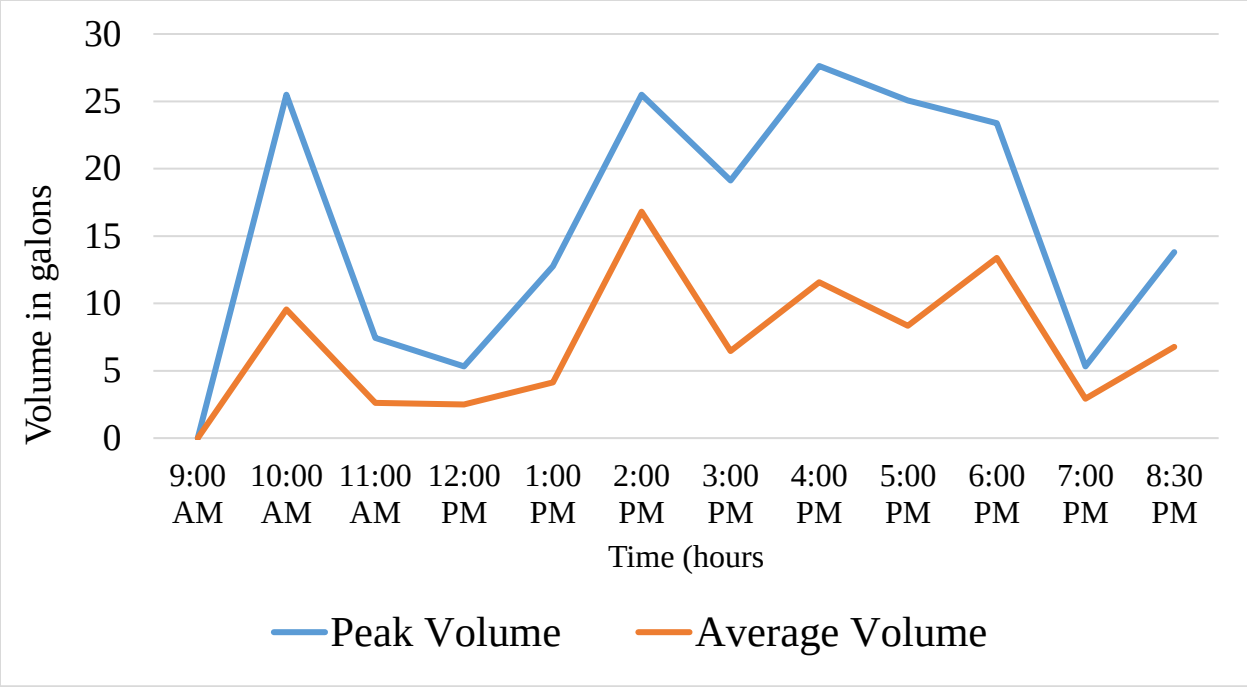

Figure 16: Diurnal grey water generation profile

3.2.2. Cooling Tower Blowdown Water

Cooling Tower Blowdown (CTBD) water used for this study was taken from a cooling tower at the HVAC setup at Pakistan Institute of Parliamentary Services, F-5, Islamabad. The cooling tower is made of 2 cells, with an estimated total refrigeration capacity of 800 refrigeration tons, and a combined operation recirculation flow of 190 m^3/hr. The cooling tower is operational for 8 – 12 hours per day during the summer season, and with a raw water make-up source of around 300 mg/L TDS concentration and a cycle of concentration maintained in the open recirculation loop of 3 – 4, the estimated CTBD water generation is 0.44 m^3/hr x 10 hrs = 4.4 m^3/day.

The open cooling water recirculating circuit is further fed by a combination of chemicals for corrosion and scale inhibition along with biocides for algal and biological growth inhibition. Phosphonate based chemistry has been implemented for the simultaneous inhibition of corrosion and scale, with scale inhibition further supplemented with HPMA based dispersant. Biocides used include chlorine and isothiazolinones. Table 7 provides important make-up and recirculating water parameters of the cooling circuit. Figure 17 shows a snapshot of the filtration apparatus at cooling tower blowdown water filtration application.

Table 7: Water parameters of Make-up and Recirculating water

Parameter	Units	Make-up Water	Recirculating Water
pH		7.5	8.5 – 9.0
Conductivity	µS/cm	410	1,340 – 2,800
P-Alkalinity	mg/L as $CaCO_3$	0	40 – 120
M-Alkalinity	mg/L as $CaCO_3$	125	340 – 750
Chloride	mg/L	35	110 – 400
Calcium	mg/L as $CaCO_3$	85	270 – 500
Magnesium	mg/L as $CaCO_3$	70	160 – 530
Turbidity	NTU		4 – 103
TDS	mg/L	286	938 – 1,960

Figure 17: Recycled Membrane filtration at Cooling Tower Blowdown water

3.3. Particle Size Characterization

Particle size analysis of the feed waters was attempted using Horiba LA300 particle size analyzer from IESE Advanced Analytical lab to estimate the particle size distribution of the particles, which is an important factor for determining the porosity of the membranes for different filtration applications. The equipment uses the principle of light scattering to estimate the size of the particles in the water. This characterization step was used for the cooling tower blowdown water only, as the particles in the grey water were visibly in the mm range, and had the potential to damage the instrument.

3.4. Membrane Performance and Fouling

Filtration runs with the membrane were carried out in dead-end and cross-flow modes. Performance of the membrane was evaluated in terms of turbidity and COD reduction to quantify the removal of particulates and organics respectively, by measuring the parameters of the feed water and comparing those with the permeate.

In between the primary testing for turbidity and COD reduction, the feed water was spiked with dairy product and cleaning solutions to simulate conditions of higher strength grey water, and the removal performance also evaluated with less rigor.

In addition to the tests for membrane performance, filtrate flux profiles were plotted against time to estimate the extent of the fouling.

3.4.1. Turbidity

Turbidity tests were performed using Hach 2100P portable Turbidimeter from the IESE Environmental Chemistry lab. The instrument operates on the nephelometric principle of turbidity measurement. The optical system, shown in Figure 18, includes a tungsten-filament lamp, a 90° detector to monitor scattered light and a transmitted light detector. The instrument's microprocessor calculates the ratio of the signals from the 90° and transmitted light detectors. This ratio technique corrects for interferences from color and/or light absorbing materials (such as activated carbon) and compensates for fluctuations in lamp intensity, providing long-term calibration stability. The optical design also minimizes stray light, increasing measurement accuracy.

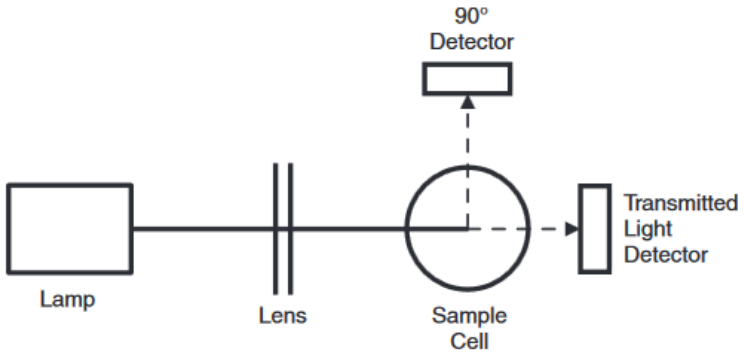

Figure 18: Optical system of Hach 2100P Turbidimeter

3.4.2. Chemical Oxygen Demand (COD)

COD was measured using the closed reflux method, in which 2.5 ml samples were refluxed with a 1.5 ml 0.1N potassium dichromate in sulphuric acid medium (3.5 ml) and the excess of dichromate was titrated against ferrous ammonium sulphate reagent in the presence of Ferroin Indicator solution, which is used to indicate change in oxidation-reduction potential of the solution and indicates the condition when all dichromate has been reduced by ferrous ion. The amount of dichromate consumed is proportional to the oxygen required to oxidize the oxidizable organic matter. All reagents used for the tests were reagent grade chemicals from the IESE Wastewater lab.

3.4.3. Silt Density Index (SDI)

SDI (Silt Density Index) is a popular test used in the industry to measure the fouling potential of primarily suspended solids in a feed water source on the RO membranes. It can used to gauge the fouling potential of the raw water and reduction in the same across any pretreatment stages to ascertain the effectiveness of the pretreatment steps. The standard SDI test method is given by the ASTM Standard D4189, and measures time required to filter a fixed volume of water through a standard 0.45 µm porosity filter with a constant pressure of 30 psi (D4189-07, 2007). The difference between the initial time and the time of a second measurement after normally 15 minutes (after silt-built up) represents the SDI value. The SDI tests were performed using SDI kit from Prime Chemicals Corporation. Testing for SDI is shown in Figure 19.

Figure 19: SDI Testing snapshot at CTBD stream

3.4.4. MFI (Modified Fouling Index)

MFI is an improvement on the SDI method, and plots the filtrate volume at intervals of 30 seconds for 15 minutes. The elapsed time t and the volume of water passing the SDI filter V are divided to plot t / V (s/L) against V (L). The slope of the curve in the intermediate segment gives the MFI value. The MFI test was also performed using SDI kit from Prime Chemicals Corporation.

3.4.5. Phosphonate

Phosphonate was tested for as residual of scale inhibitor used for the cooling tower chemical treatment program. This was measured using La Motte 7625-01 mobile test kit with support of Prime Chemicals Corporation. The method principally used titration with 0.00132M Thorium Nitrate of 10 ml sample along with Sodium Thiosulfate and Chrome Azurol S Indicator to determine the concentration of phosphonate present in the water.

3.4.6. Microbial Analysis

The ability of the converted membrane to remove microbial contamination for CTBD feed water was evaluated by comparing the Most Probable Number (MPN) of total coliform and E.coli in the feed water with that in the filtrate. The MPN test was carried out using the multiple tube method by an accredited laboratory (Islamabad Diagnostic Center) to which the testing was contracted.

Chapter 4: Results & Discussion

4.1. Membrane Conversion

After chemical cleaning and hypochlorite exposure of 300,000 ppm.h, the two end-of-life RO membranes were tested for permeability and salt rejection. The Lewabrane B085 HF 4040 membrane attained a relatively higher permeability of 35.4 lmh/bar than the DOW Filmtec BW30-400 membrane permeability of 27.0 lmh/bar. Plots of membrane flux against the Transmembrane Pressure (TMP) are shown in Figure 20. In terms of salt rejection, for both membranes, the salt rejection after the cleaning and conversion process was below 5%.

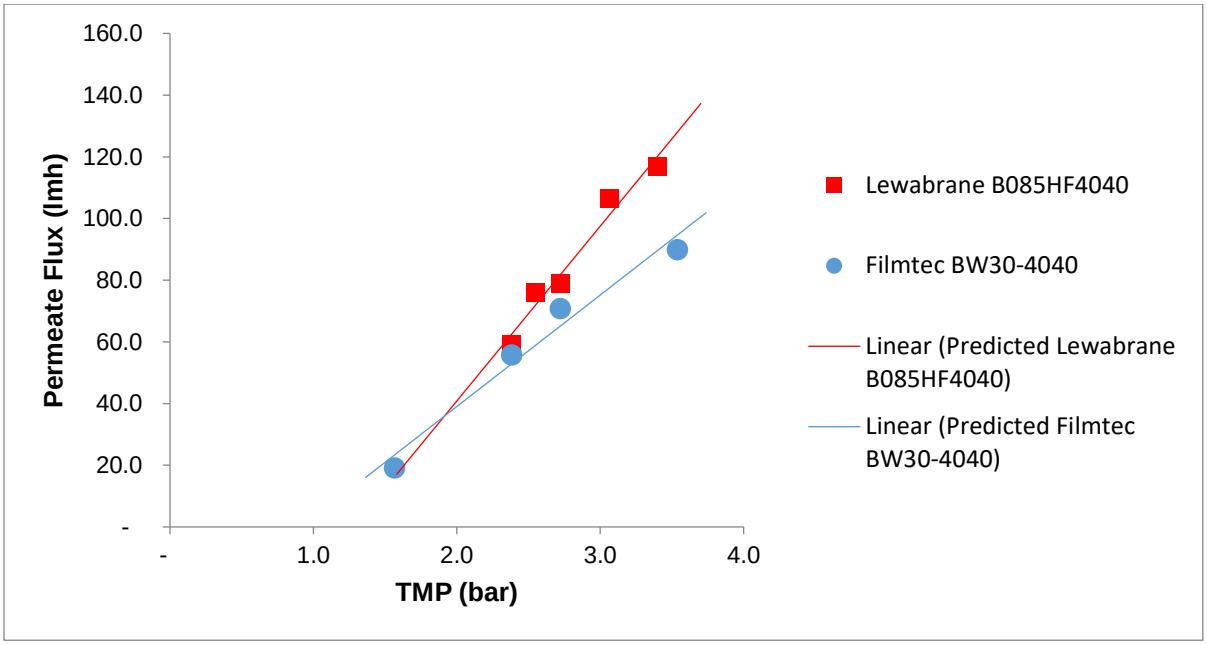

Figure 20: Membrane flux vs Transmembrane Pressure for the converted membranes

The relative variation among the converted membranes in terms of permeability can be attributed to the different types of foulants that may have deposited on the membrane during operation, effectiveness of the cleaning steps in removing those foulants, and membrane storage conditions after being discarded, the degree and pressure of pre-wetting and manufacturer specific materials and properties (Lawler et al., 2013). Moreover, the membrane permeability attained for the discarded RO membranes is significantly less than the 170 lmh/bar figure reported by Lawler et al. as they used virgin instead of actual end-of-life RO membranes for the conversion process.

4.2. Membrane Performance with LGW Feed Water

Testing of membrane performance with LGW feed water was based on the removal of particulates, quantified by turbidity, and removal of organics, quantified by COD.

4.2.1 Turbidity Removal

With the LGW feed water, the membrane was operated in both the cross-flow and dead-end modes. During operation in both modes, the converted membranes demonstrated turbidity removal in excess of 95%, providing consistent filtrate turbidities less than 1 NTU. Figure 21 shows the feed water and filtrate turbidities for this stream. The LGW stream showed a high degree of variance, primarily due to spike tests, discussed in succeeding sections, and the inflated datasets have been discounted as outliers.

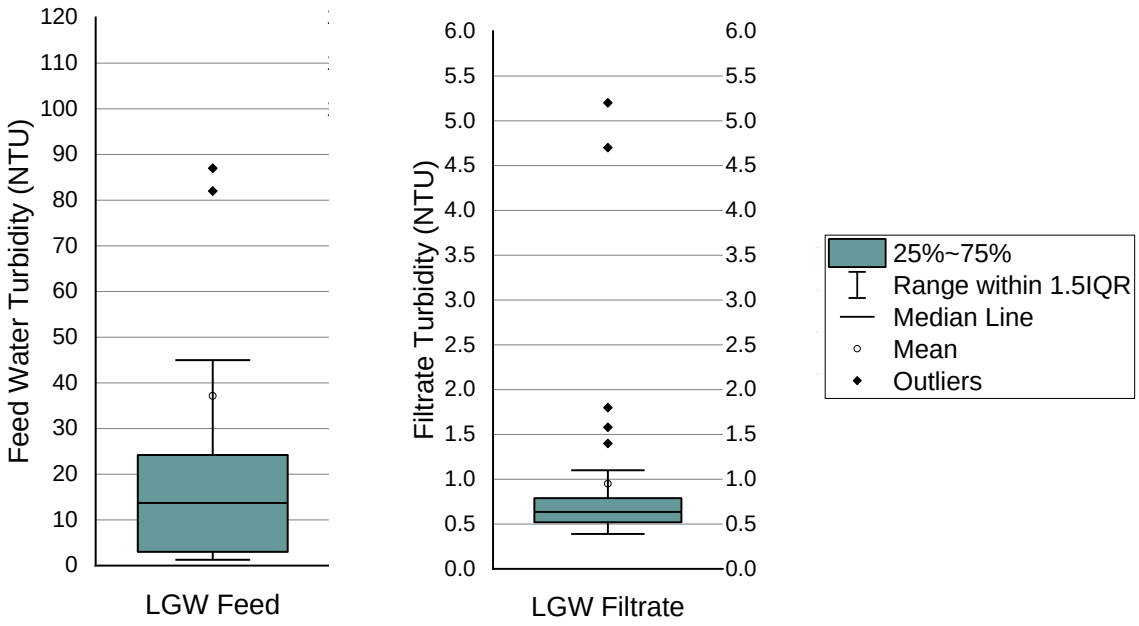

Figure 21: Feed water and filtrate turbidity for LGW stream

Tables 8 further provides a statistical summary of the average feed and filtrate water turbidities and average turbidity reduction for the LGW stream.

Table 8: Average LGW feed and filtrate turbidities during filtration runs

	Feed (NTU)	**Permeate (NTU)**
Average Turbidity	37.15	0.95
Average Removal		97.4%

4.2.2 COD Removal

The box-and-whisker plot for the reduction in COD (Chemical Oxygen Demand) is shown in Figure 22. In general, the membrane attained COD reduction of around 70% with the feed water COD values varying around 100 mg/L. Table 9 summarizes the average data with and without outliers.

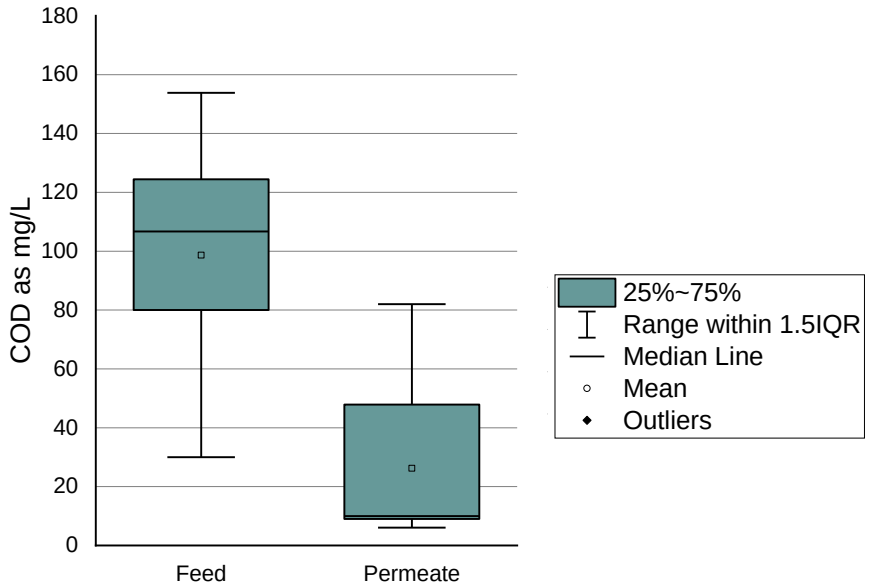

Figure 22: Feed and Permeate water COD during filtration test runs

Table 9: Average feed and permeate COD during filtration runs

	Feed (mg/L)	**Permeate (mg/L)**
Average COD	118.3	51.9
Average COD (Excluding Outliers)	98.7	26.4
Average Removal		73%

"Outliers" have specifically been addressed as these were the results of spike tests. In these tests, the feed water was spiked to a feed COD value of 490 mg/l with the addition of a dairy product to simulate feed water properties of high strength grey water. In that scenario, the reduction in COD was only 6%. This suggests the requirement for more rigorous testing if high strength grey water (HGW) is to be considered for treatment through recycled membranes. Figure 23 shows the average COD reduction including the outliers introduced by the spike tests, COD reduction in the case of the spike tests, and the average COD reduction with the outliers excluded from the dataset.

Another spike test was carried out in which the feed water was spiked with residual of alkaline cleaning of the second membrane to simulate the effect of cleaning wastes and detergents. Although, the feed COD did not register any spike, a turbidity value of as high as 514 NTU was recorded, and the filtrate turbidity was again less than 1 NTU.

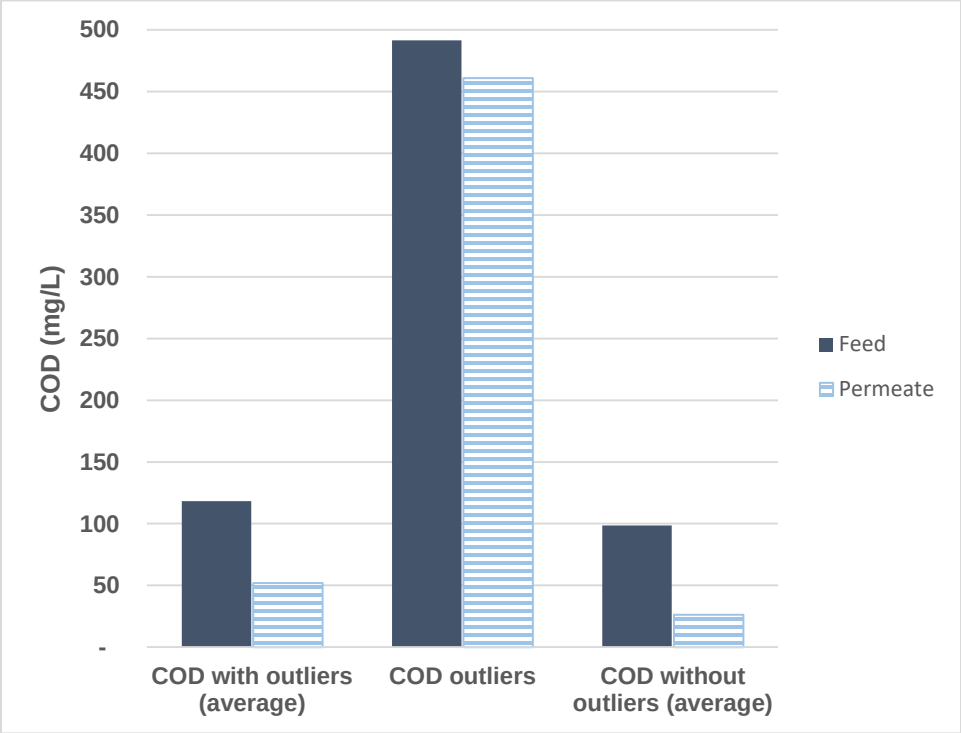

Figure 23: COD reduction including and excluding effect of spike test

4.3. Membrane Performance with CTBD Feed Water

Testing of membrane performance with CTBD feed water was based on the removal of particulates, quantified by turbidity. Overall reduction of the fouling potential of the filtrate was quantified by testing for SDI and MFI. Tests for total coliform and E.coli of feed and filtrate were also performed to study the microbial rejection performance of the membrane.

4.3.1 Turbidity Removal

Figure 24 shows the feed water and filtrate turbidities for the CTBD stream. While the turbidity removal for this stream was also consistently above 90%, the filtrate turbidity was relatively higher than that achieved for the LGW feed water. For the CTBD filtrate, the relatively higher turbidity values were understood to be as a consequence of carryover of the HEDP-HPMA corrosion and scale inhibitor being dosed into the cooling tower. This is supported by the limited phosphonate removal and simultaneously low SDI values of the filtrate from CTBD feed stream as discussed in the succeeding sections.

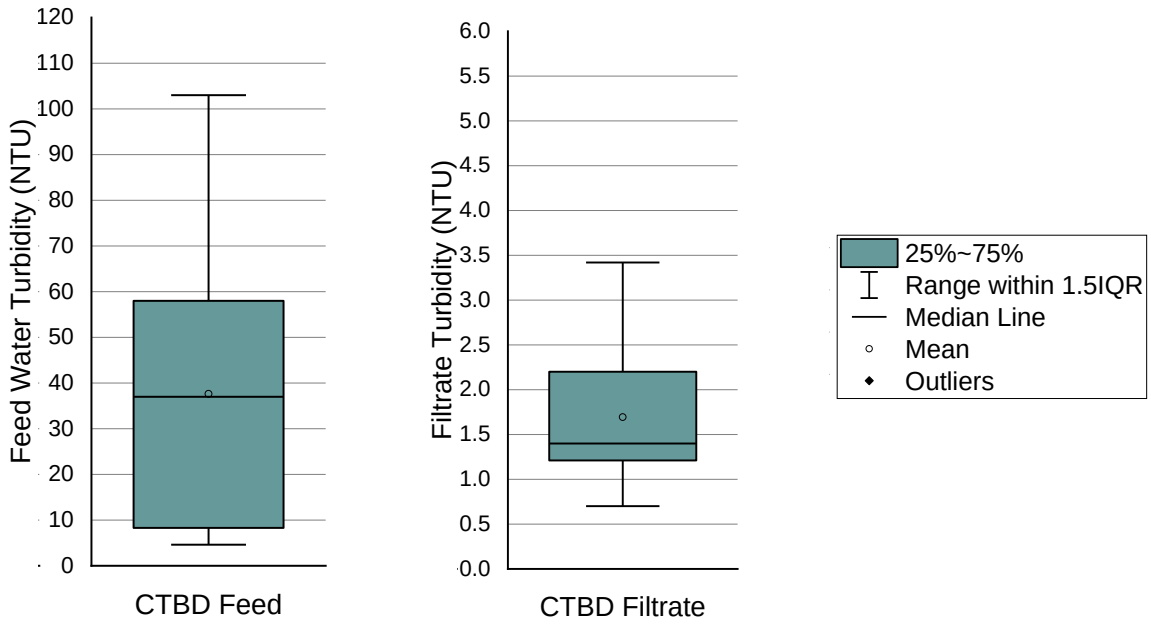

Figure 24: Feed water and filtrate turbidity for CTBD stream

Table 10 further provides a statistical summary of the average feed and filtrate water turbidities and average turbidity reduction for of the CTBD stream.

Table 10: Average CTBD feed and filtrate turbidities during filtration runs

	Feed (NTU)	**Permeate (NTU)**
Average Turbidity	37.62	1.69
Average Removal		95.5%

4.3.2 Phosphonate Removal

The concentration of phosphate in feed and filtrate water as HEDP as mg/L is plotted in Figure 23 in the form of a box plot. The decrease in the average phosphonate content is statistically significant with a one-tail p value of 2×10^{-4}, and an average removal rate of around 19.9% from an average recorded phosphonate level of 39.1 mg/L in the feed to 31.1 mg/L in the filtrate. This suggests that only a portion of the phosphonate is removed through the membrane, and that the rest carries forward through the membrane and may potentially be responsible for the faint yellow hue of the filtrate for CTBD water stream.

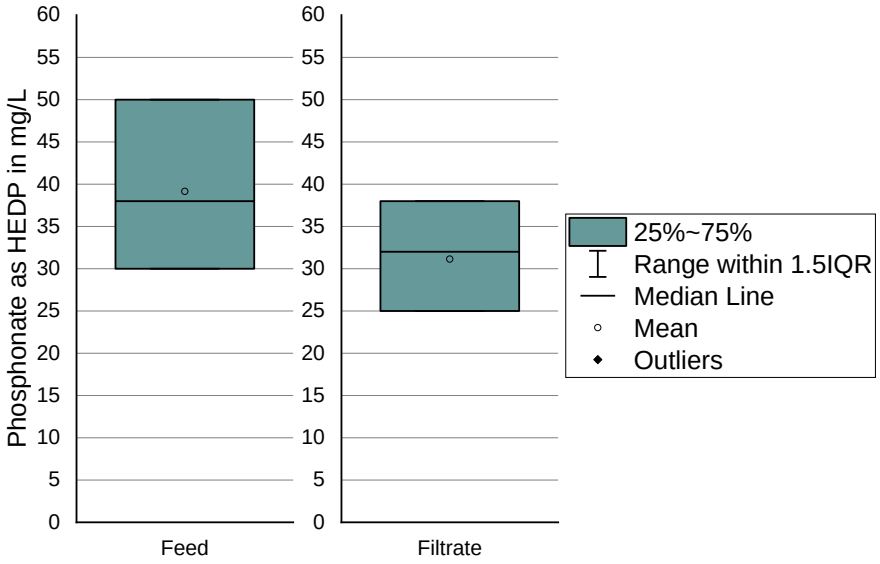

Figure 25: Phosphonate reduction from CTBD stream

4.3.3 Particle Size

Particle size distribution of the cooling tower blowdown water, shown in Figure 26, has a distribution from 5 μm to 600 μm, with a median value of 276 μm. Figure 27 and Table 11 shows the screenshot of the particle size analyzer graphical user interface, which shows a 95.5% transmittance for the feed water (cooling tower blowdown water) and a 100% transmittance for the filtrate water, demonstrating that the filtrate water maximum particle size is below the 0.1 μm

minimum detection limit of the analyzer, confirming at most a 0.1 µm value as the absolute porosity of the converted membranes. Theoretically, this value should be sufficient to remove all species of bacteria by size exclusion.

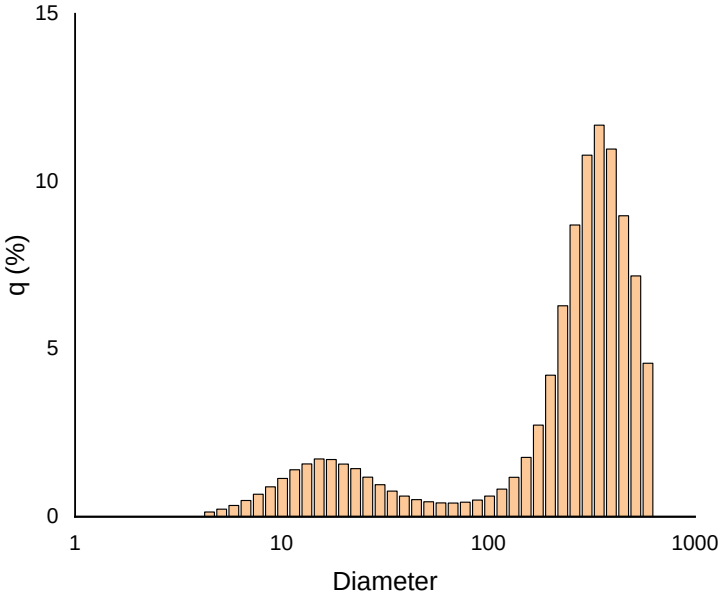

Figure 26: CTBD Water Particle Size Distribution

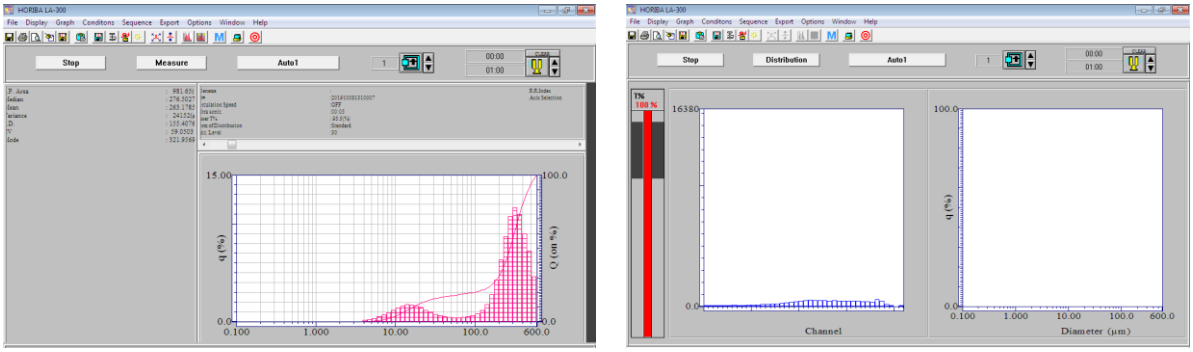

(a) Feed Water (b) Filtrate Water

Figure 27: Horiba LA300 Screenshot for transmittance for feed and filtrate water

Table 11: Particle Size Analysis summary of feed and permeate

	Feed (mg/L)	**Permeate (mg/L)**
Laser Transmittance	95.5%	100.0%
Minimum Particle Size (µm)	4.5	N/A
Median Particle Size (µm)	276.5	N/A
Maximum Particle Size (µm)	600.0	< 0.1

4.3.4 SDI

Filtrate silt density index (SDI) values were invariably found to be less than 1.0, which represents otherwise excellent water quality for feed to RO membranes in CTBD recycling applications with a very low fouling potential due to particulates. The SDI test subjected the membrane filtrate to 0.45 micron filter paper at a pressure of 30 psi, and noted the time taken to filter 500 ml before and after 15 minutes of filtration. As with TSS measurements using the 0.45 micron filter, the filter paper after filtration carries a residue of the particulates, which is often visible for waters with appreciable suspended solids concentration. In the case of the CTBD filtrate in the current study, the SDI filter was further free from visible residues, and indicated very good filtrate water quality. A close up snapshot of an SDI filter is shown in Figure 28.

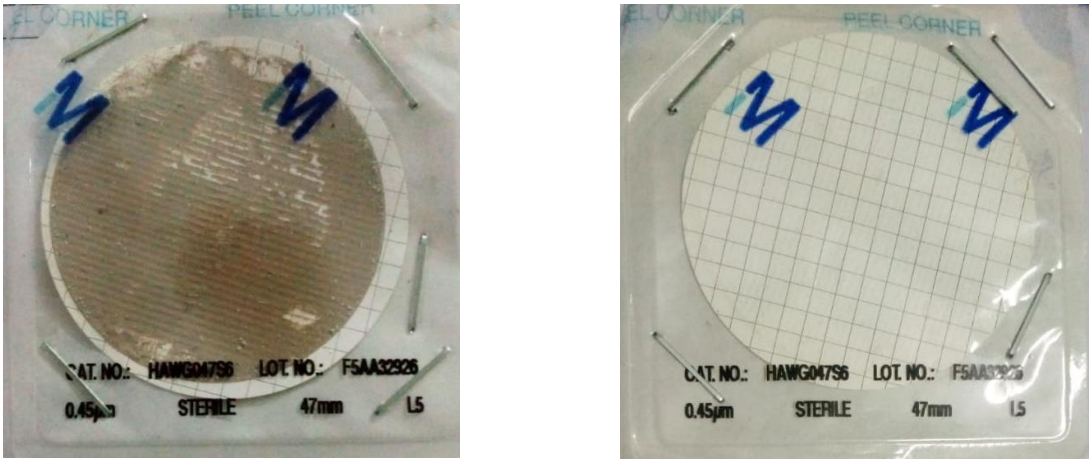

(a) Feed water (b) Filtrate

Figure 28: SDI filter after use with CTBD before and after membrane filtration

4.3.5 MFI

The CTBD filtrate MFI value was calculated by plotting t / V (s/L) against V (L), and finding the slope of the intermediate section of the curve. The plot is shown in Figure 29. The slope of the curve between V = 3.2L and V = 10.8L, and hence the MFI value, was found to be 0.109 with an R^2 value of 0.9995. This compares favorably with a benchmark MFI upper limit of 1.0 which is generally recommended for RO feed waters.

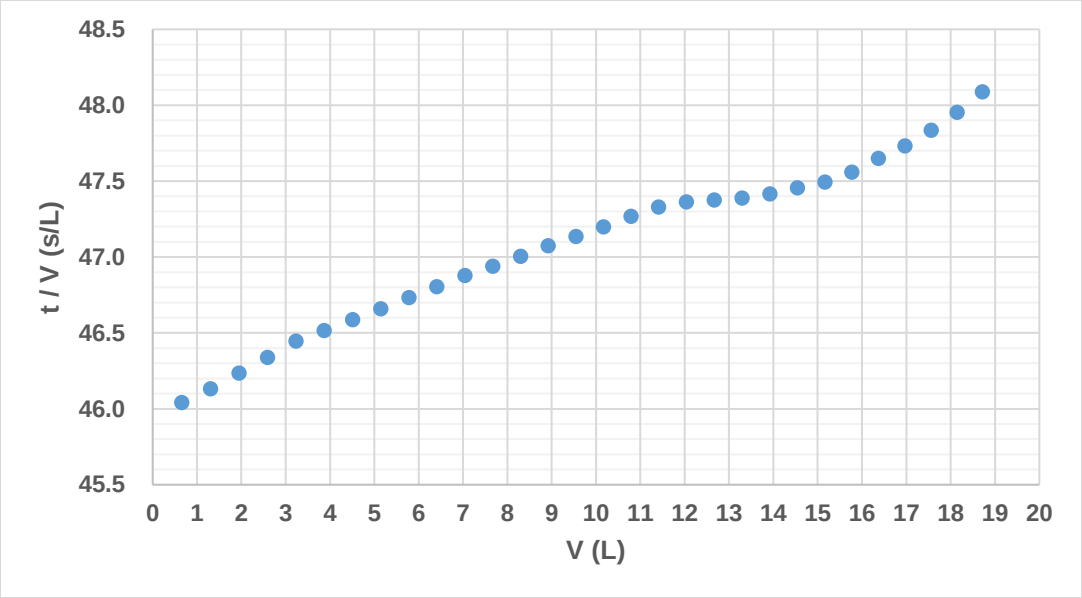

Figure 29: Plot of t/V vs V for estimation of MFI

4.3.6 Microbial Analysis

The converted membrane capability of rejecting microbial contamination was also studied. Quantification was carried out using MPN of total coliform and E.coli for the CTBD stream. Before microbial tests were conducted, membrane was subject to a sanitization procedure to ensure that the results were representative of the membrane's own microbial rejection and discounted prior growth on the filtrate side during earlier filtration and backwash runs. The sanitization procedure included recirculation of a combination of an oxidizing (sodium hypochlorite) and a non-oxidizing biocide (isothiazoline with 1.5% active concentration) at dosages 500 ppm for 1 hour).

The membrane reduce the MPN of the total coliforms as well as the E.coli from above log-3 (1.1 x 10^3 CFU/ml) to 0 CFU/ml. This is consistent with the expected removal of theoretically all microorganisms by size exclusion by even the maximum expected membrane porosity of 0.02 µm.

4.4. Membrane Operation

4.4.1 Operational Mode

In all the filtration runs, the membrane feed, concentrate and permeate pressures, in addition to the permeate flow were logged, and the data were used to plot the permeate flux decay due to membrane fouling.

During initial operation of the converted membrane at the grey water pilot application, the membrane was subjected to filtration runs in both the cross-flow and dead-end modes. Figure 30 shows the normalized flux decay profiles for the three operational modes: (i) dead-end mode, (ii) cross-flow mode at 55% recovery and (iii) cross-flow mode at 10% recovery for 300 minutes of operation. The cross-flow mode at 10% recovery entailed use of high cross-flows of up to 3.6 m^3/hr, slightly below the recommended values as per Table 3, to allow simultaneous flushing of the membrane as a flux maintenance strategy. It can be seen that this cross-flow was able to practically eliminate loss of flux in comparison to the dead-end mode. An intermediate recovery of 55% was also trialed, but only partially reduced the flux decay. In the dead-end mode, the flux decayed to 60-70% of the initial flux much rapidly, but a portion of that was recoverable through use of simple backwashing.

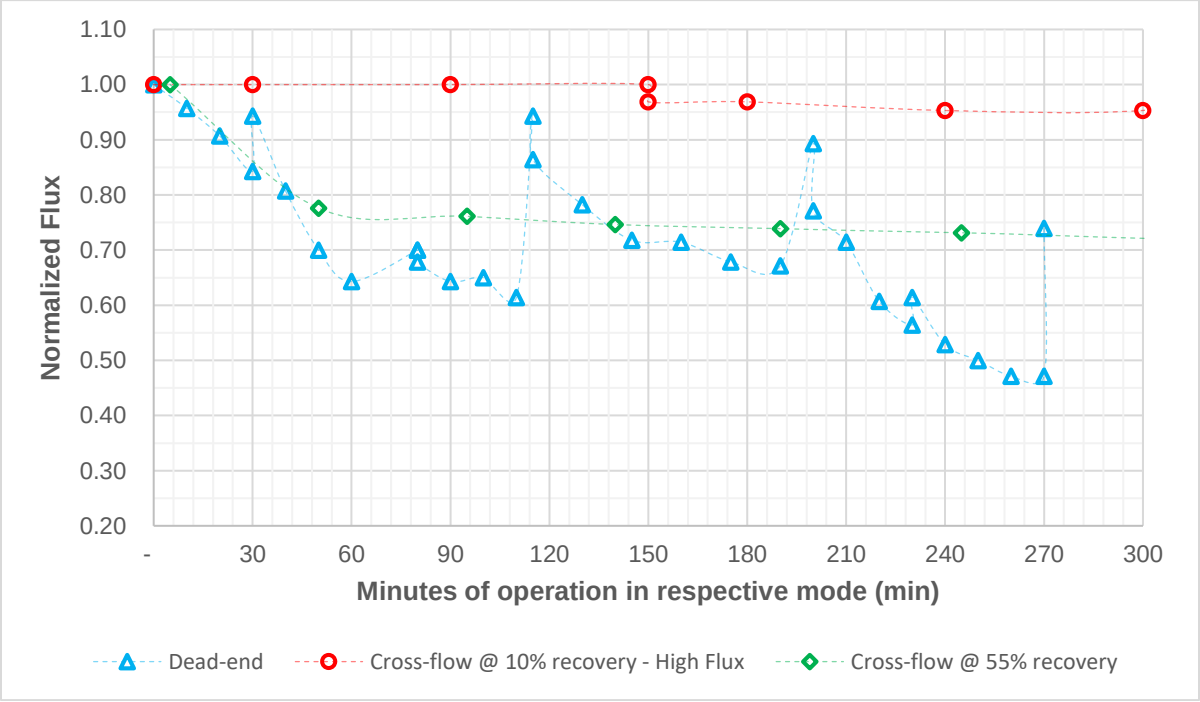

Figure 30: Flux decay profiles in different operational modes

While the filtrate flux in cross-flow mode at 10% recovery practically remains stable during longer filtration runs, operation at such a low recovery entails an obvious higher cost of filtration because only 10% of the total pumped water is actually filtered. Even for the intermediate recovery scenario, only 55% of the total pumped water is filtered, necessitating twice the pumping cost for the same volume of water filtered in dead-end mode. A higher recovery scenario using 90% recovery was also trialed, and the flux profile is plotted in Figure 31 with a profile for dead-end mode, showing little to no improvement in flux decay. These results suggest that high cross flows are required to allow operation without significant flux decline, and low cross flows have little impact in reducing fouling leading to flux decay. Simultaneously, high cross flows have an obvious adverse impact on the economics of filtration. Correspondingly, all subsequent filtration runs were attempted in dead-end mode, and alternative flux enhancing strategies were considered, which are discussed in section 4.4 in further detail.

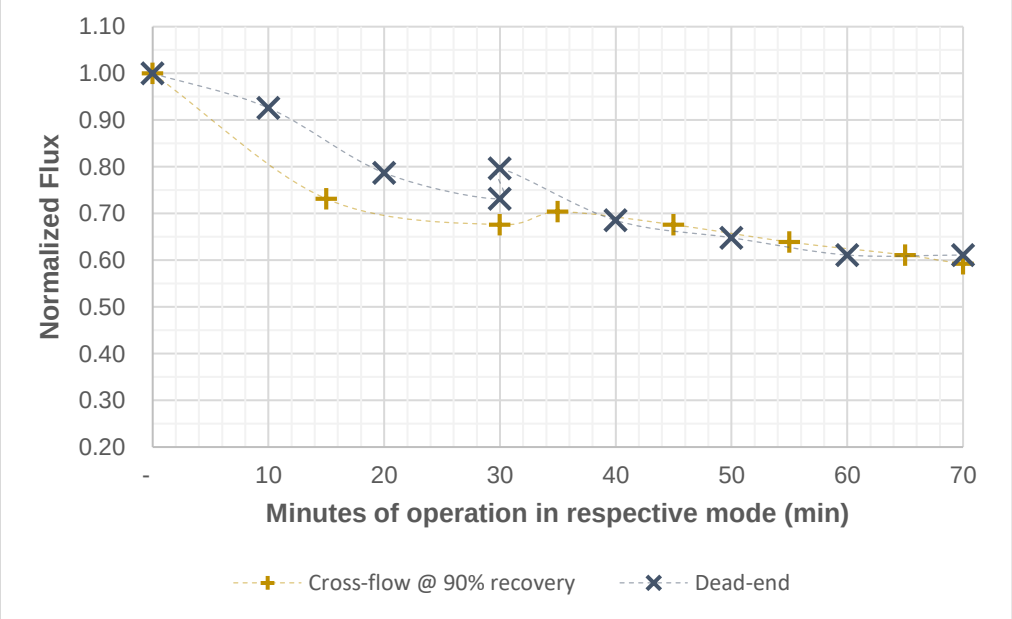

Figure 31: Flux decay profile for dead-end with high recovery cross-flow

4.4.2 Operational Flux

In the discussion on converted membrane permeability in Section 4.1, membrane filtrate flux is plotted against the TMP in Figure 20. Noting that typical ultrafiltration applications are carried out at a TMP of around 2 – 4 bars, the corresponding filtrate flux in the range of 40 – 120 lmh can be expected at start of filtration runs. Again, this range corresponds with typical filtrate flux for conventional ultrafiltration applications.

Although initial filtrate flux of as high as 100 lmh was also trialed for shorter durations, operation at a lower flux allowed more sustainable operation for longer runs supported by regular backwash. Figure 32 plots the filtrate flux for membrane operation with CTBD feed water for over 600 minutes of operation and an initial flux of around 65 lmh. The figure shows relatively sustainable operation with almost total recovery of flux through simple backwash.

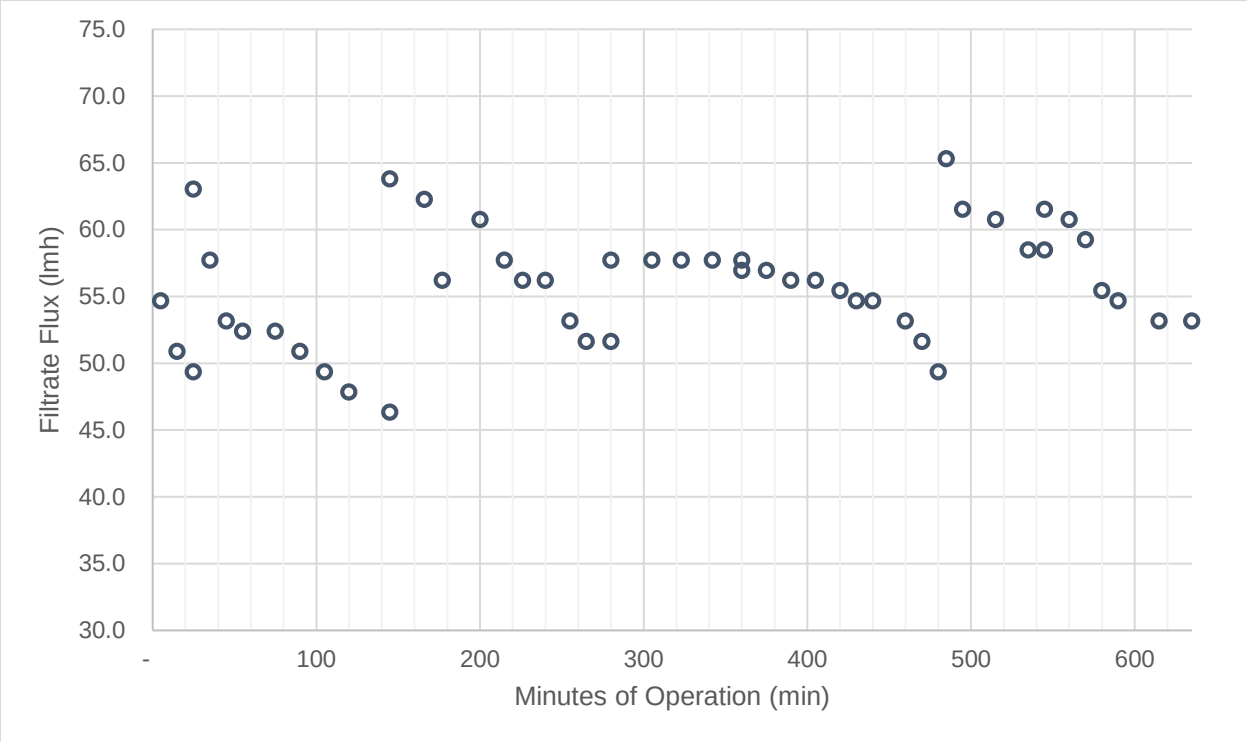

Figure 32: Filtrate Flux with CTBD feed for over 600 minutes of operation

4.4.3 Operational Cycles

Figure 32 also demonstrates that normal backwash was able to fully recover flux after 60-90 minutes of operation in filtration mode. The normal backwash sequence used throughout involved alternation of backwash and forward flush similar to that in typical ultrafiltration membrane applications. Furthermore, membrane manufacturers typically suggest a backwash sequence after between 20 and 60 minutes of operation.

4.5. Membrane Fouling

4.5.1 Flux decline due to Fouling

Figures 30 through 32 give an idea of the flux decline profiles across the converted membrane, which can be attributed to membrane fouling. This section looks at the phenomenon more closely and develops correlation with the recognized empirical fouling models. In doing so, the flux was plotted against the time of the filtration run. The corresponding values of $ln(J), \frac{1}{J}, \frac{1}{\sqrt{J}}$ and $\frac{1}{J^2}$ were linearly regressed with time to explore correlation with the CPB, SPB, IPB and CF models respectively. These values are plotted against time for one of the filtration runs with LGW feed in Figure 33 followed by the flux profile along with the predicted values for each of the model in Figure 34.

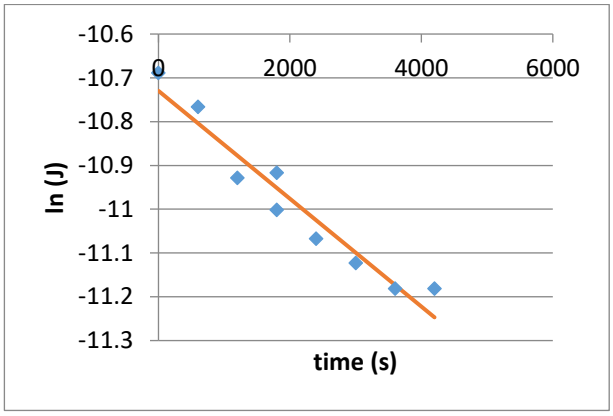

(a) Complete Pore Blocking model with R^2=0.93

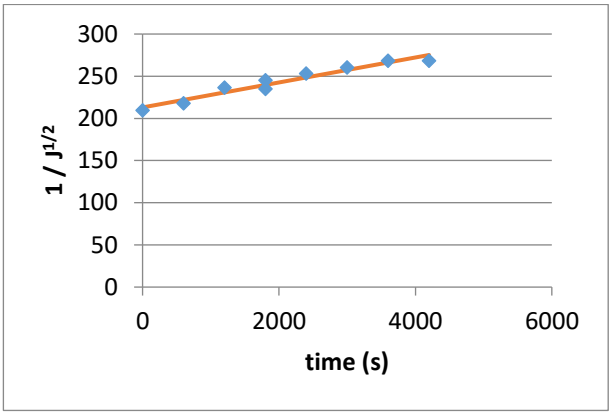

(b) Standard Pore Blocking model with R^2=0.94

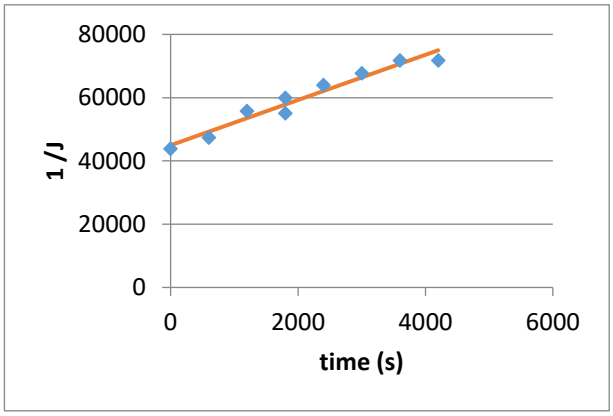

(c) Intermediate Pore Blocking model with R^2=0.95

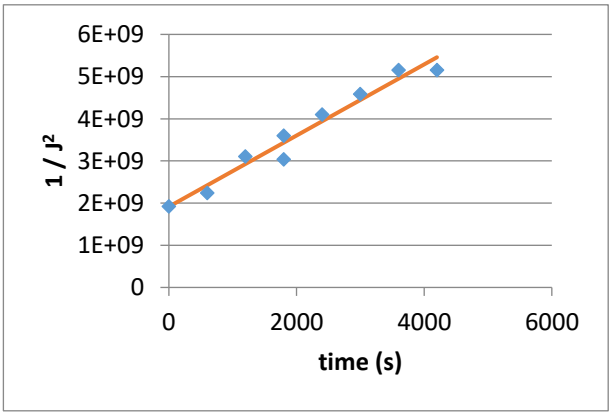

(d) Cake Filtration model with R^2=0.95

Figure 33: Linear Regression curves of flux (J) with fouling models

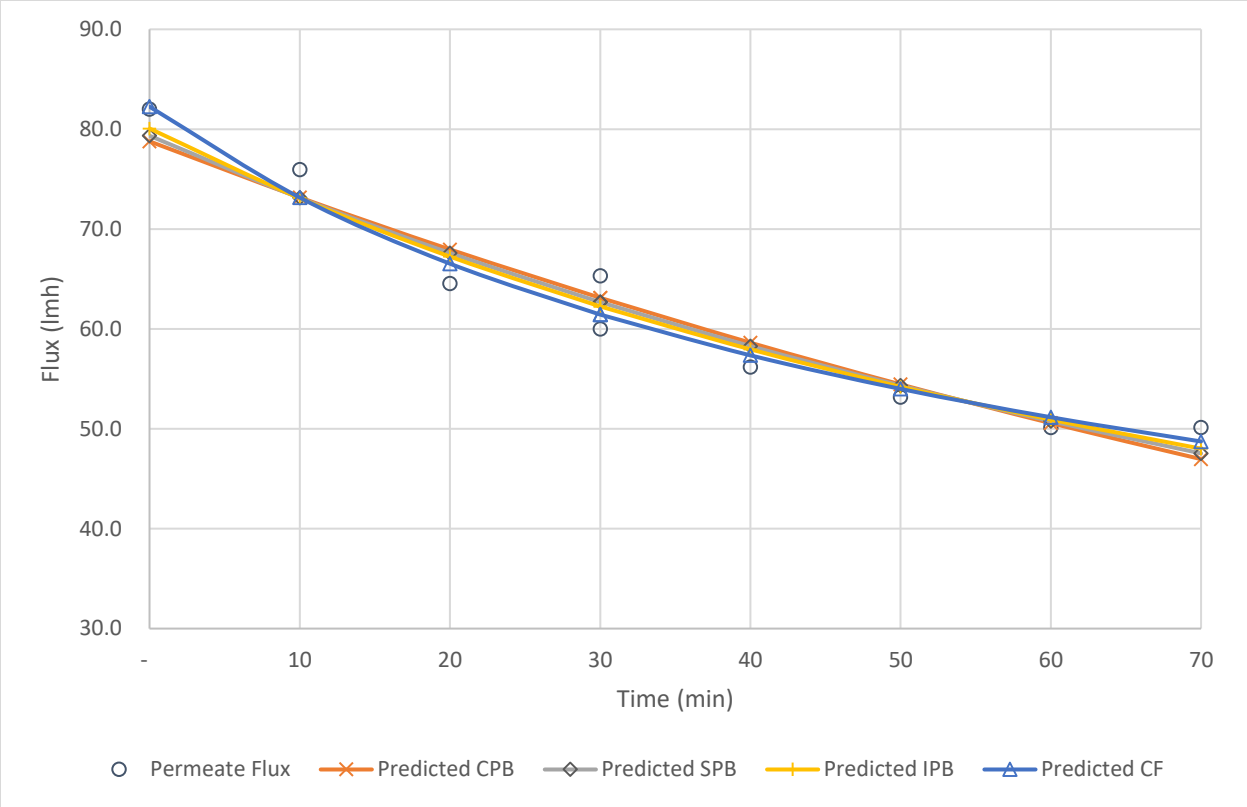

Figure 34: Observed vs Fouling model-predicted flux profiles

Figures 35 through 38 plot the experimental data with the CPB, SPB, IPB and CF models for multiple filtration runs with both LGW and CTBD feed water streams. The coefficients of correlation R^2 can be seen to vary between 0.87 and 0.96, which are within the limits of acceptability for previous similar studies using conventional ultrafiltration membranes (Salahi et al., 2010; Vela et al., 2008).

The data indicate that, in general, feed water turbidity directly affects the coefficient for the respective run, highlighting the impact of particulates in feed water on membrane fouling. The LGW streams' flux decline appears to be relatively accelerated as compared to the CTBD. The most obvious reason for this appears to be the larger particulate size of the suspended contaminants in the LGW feed. Furthermore, from among the two streams, application of normal backwash appeared to restore the flux for the CTBD stream much efficiently as compared to the LGW stream, indicating that fouling in CTBD stream may exclusively be due to particulates, while that in the LGW stream may have a portion of fouling due to organics or biofouling, for which use of CEB and/or CIP was seen to restore flux as discussed in the next section.

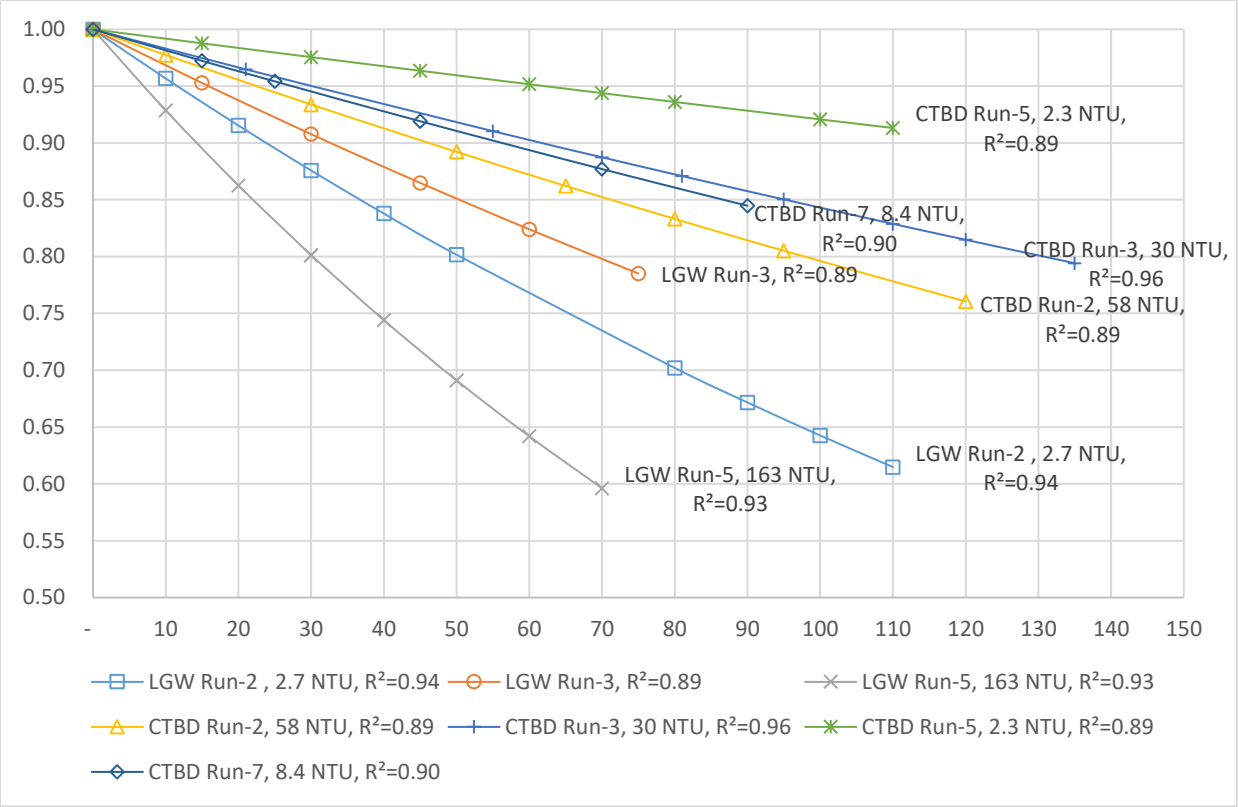

Figure 35: Filtrate flux predicted by CPB model

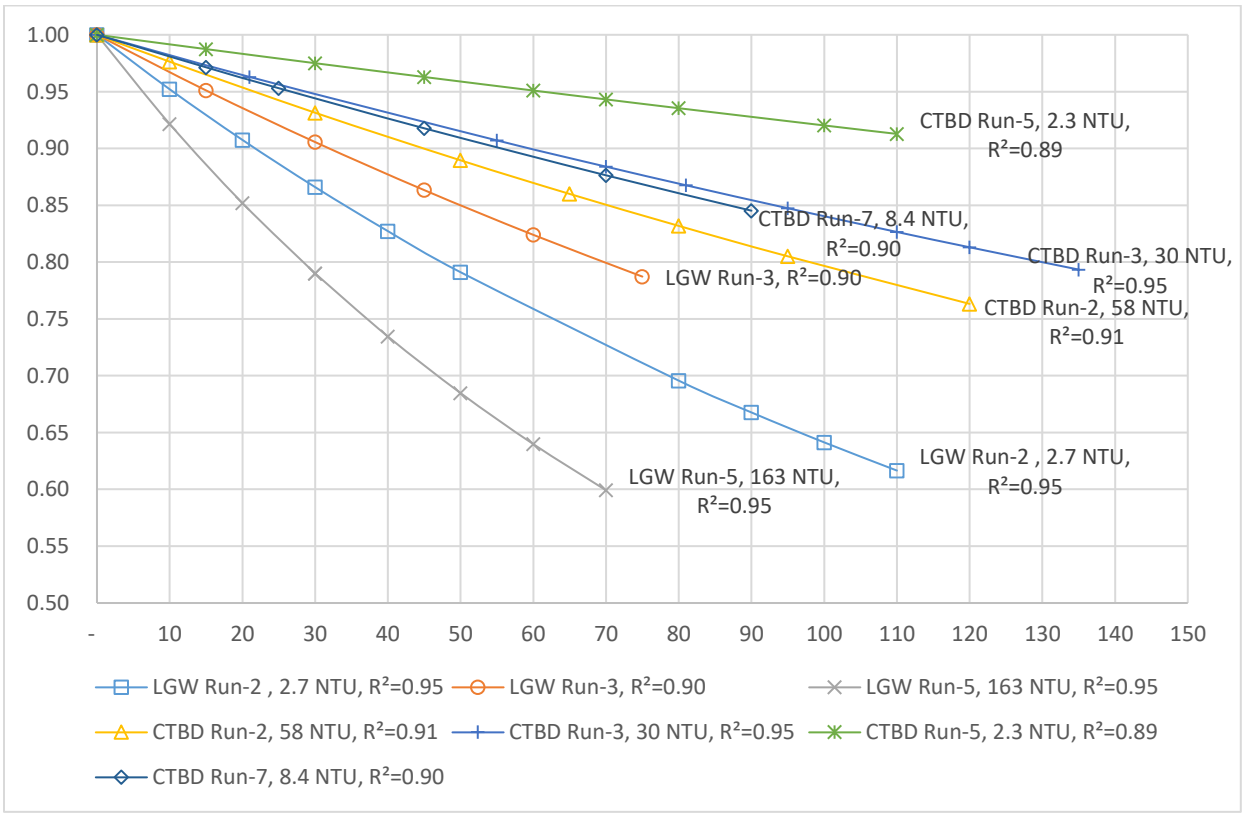

Figure 36: Filtrate flux predicted by SPB model

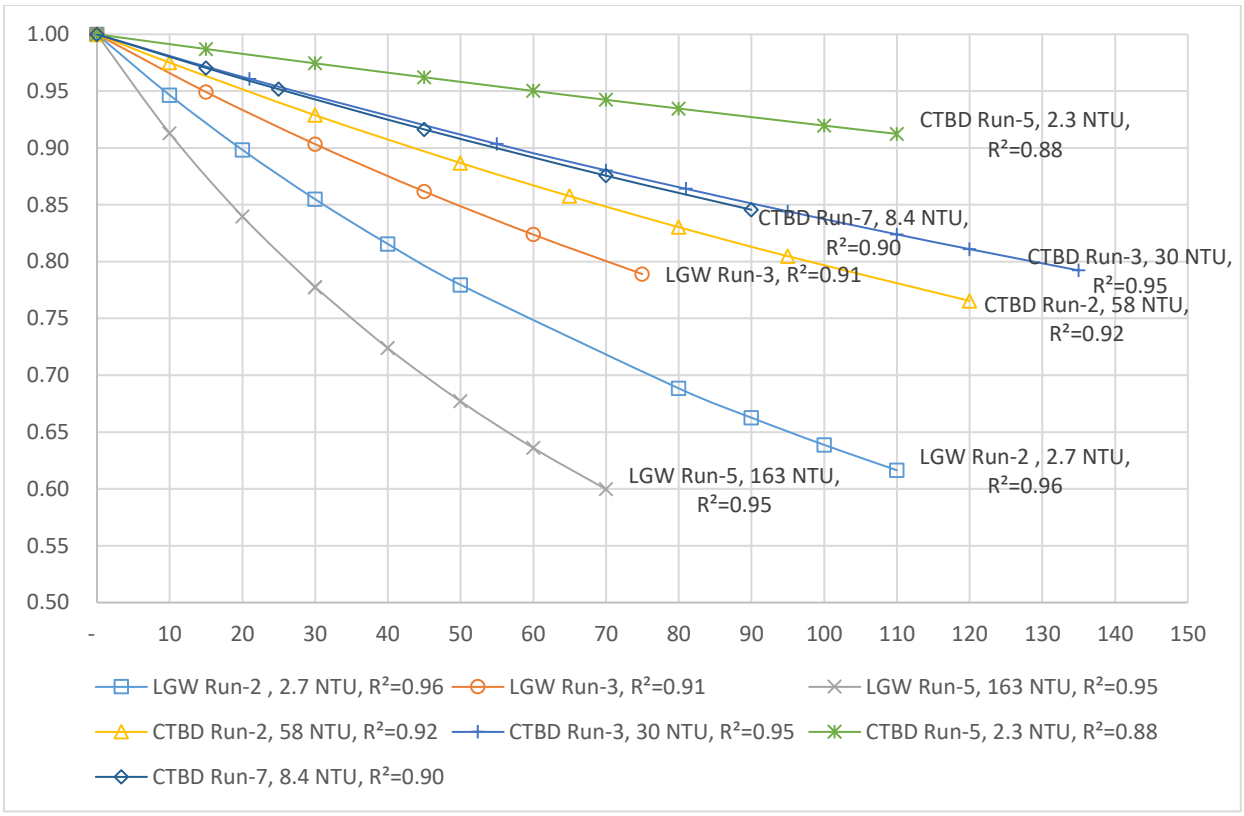

Figure 37: Filtrate flux predicted by IPB model

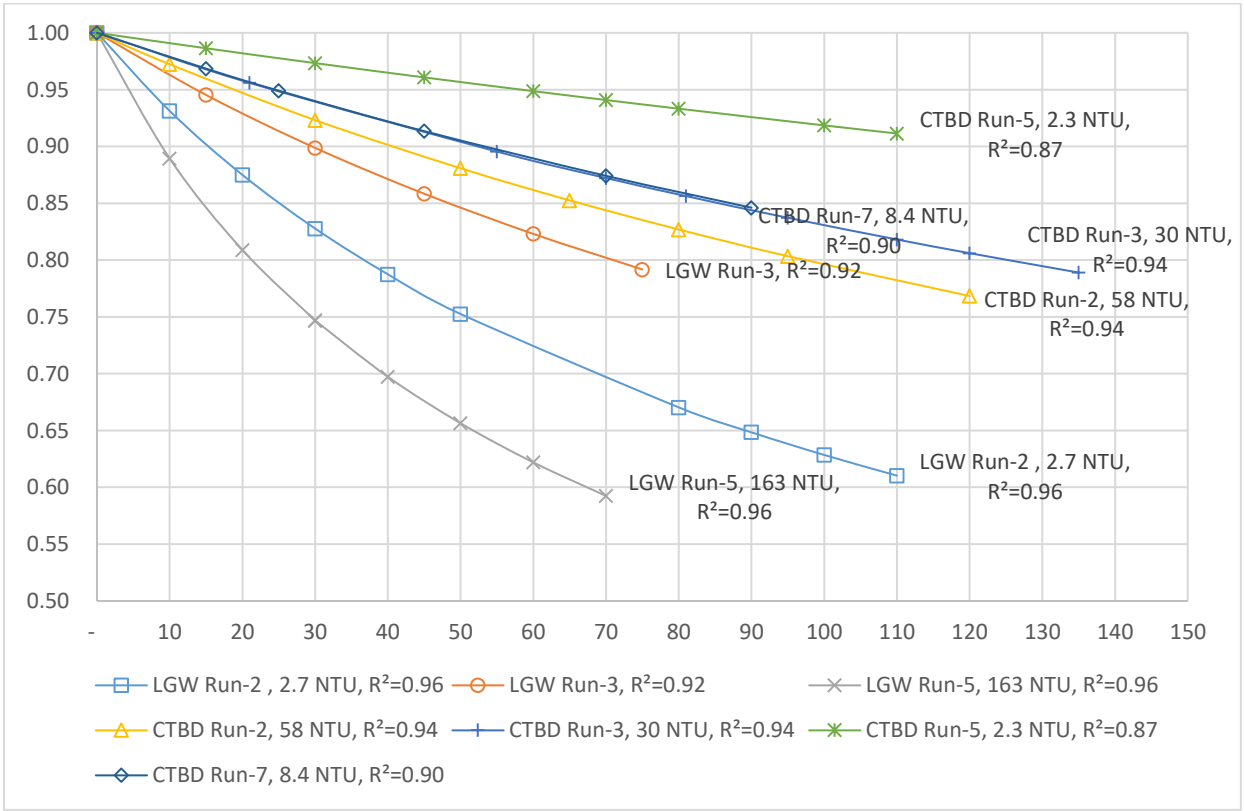

Figure 38: Filtrate flux predicted by CF model

4.5.2 Flux Recovery

Figure 32 shows the plot of membrane filtrate flux decay for multiple filtration runs in dead end mode for CTBD feed water with each run succeeded by steps of backwashing and forward flushing. The same for LGW feed is shown in Figure 39.

Figure 39 suggests that a portion of the fouling is readily reversible in that the flux is restored by simply backwashing the membrane, and a portion of the fouling is not readily reversible in that the flux is not restored to the value at the start of the filtration run with backwashing alone.

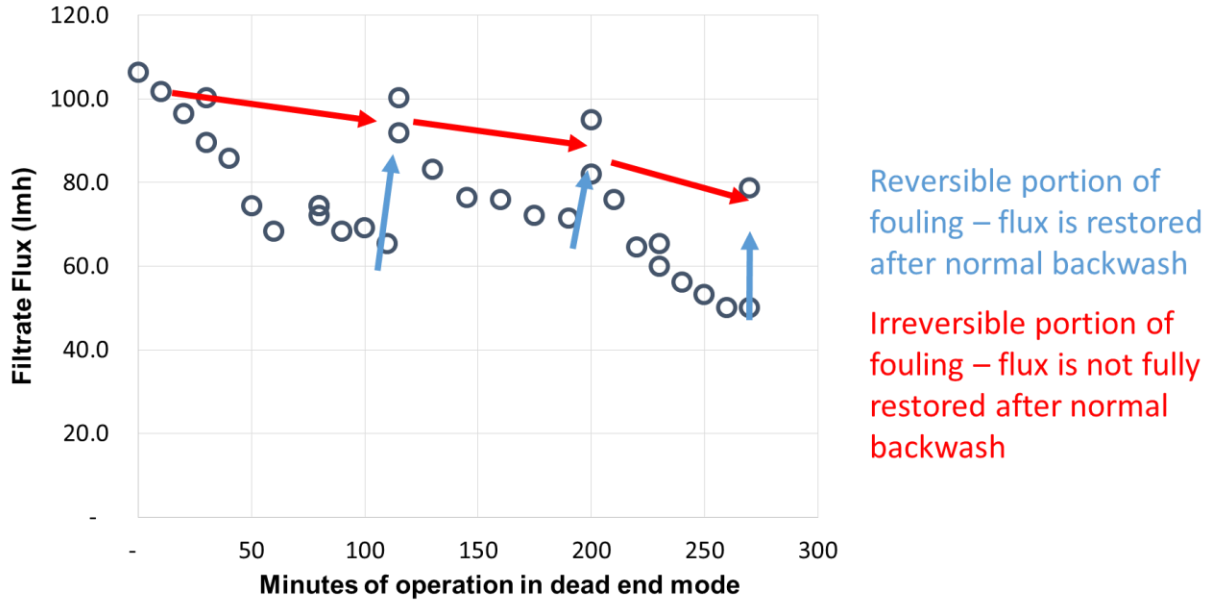

Figure 39: Permeate flux decline in multiple dead-end filtration runs

In realization of the fact that fouling is expected to be a major concern for recycled end-of-life RO membranes, different antifouling techniques beyond the simple backwash were attempted. A combination of CIP (Clean in Place) and CEB (Chemically Enhanced Backwash) was used to clean the membrane. Both the CIP and CEB are commonly used recovery tools for ultrafiltration membranes in commercial use that use chemicals to remove the foulants from the membrane surface as a recovery tool. First, the membrane was backwashed with ultrafiltration filtrate water at the end of a filtration run. The backwash was able to restore the flux to 88% of the flux at the start of the filtration run.

The membranes was then cleaned through a combination of CIP and CEB with a chemical concentration in the same range as that used for the pre-converted RO membrane as documented in the preceding sections. This was able to bring about a further recovery of 7% was achieved. The results are shown in the waterfall diagram in Figure 40.

While the short term residual irreversibility of 4.6% does appear as a cause for concern for sustainable membrane operation, it is emphasized that the feed water was incident on the without any upstream prefilter. In typical UF applications, upstream straining to between 100 and 500 microns is generally recommended (Crittenden et al., 2012). For the current feed water, the particle size was well in excess of the 600 micrometer upper detection limit of the available particle size analyzer to allow quantification. The particles were noted to be visibly in the millimeter range, which may have led the membrane to undergo accelerated particulate fouling.

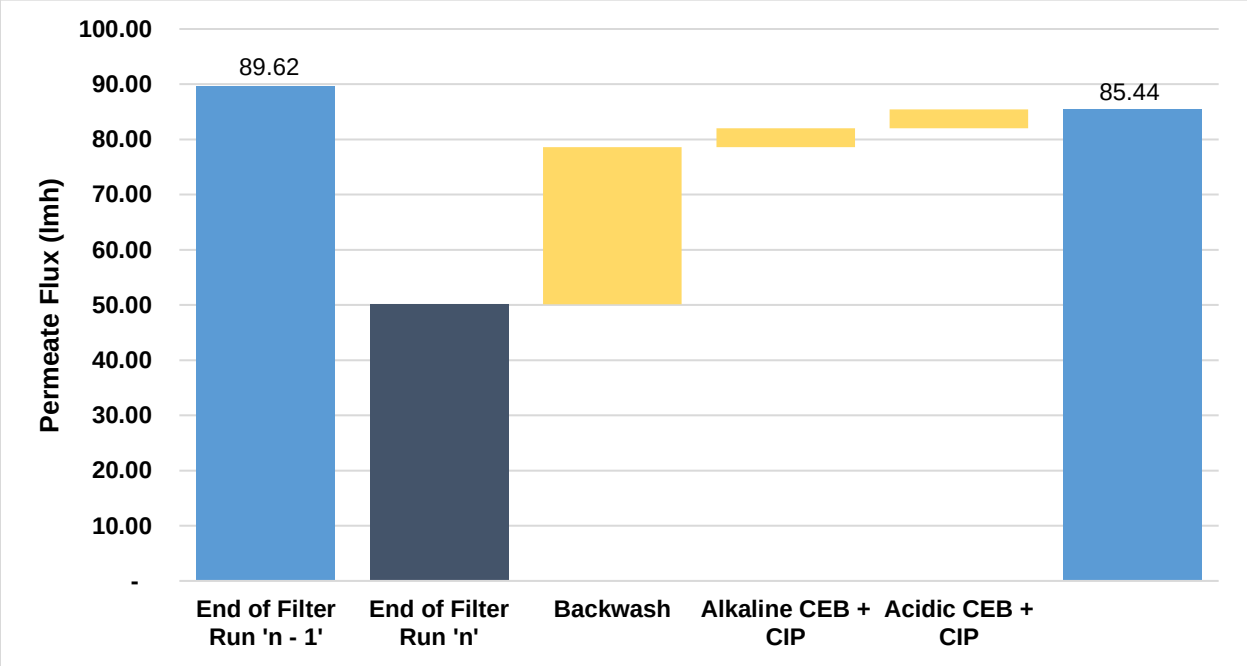

Figure 40: Permeate flux recovery through backwash and chemical cleaning

Furthermore, as covered in section 4.3.1, the inhibitory effect on fouling of inducing a cross flow velocity to the operational mode was investigated. A cross flow of 3.6 m^3/hr, corresponding to a recovery of around 10%, was able to almost eliminate flux decline in 10 hours of operation.

Chapter 5: Conclusions & Recommendations

5.1. Conclusion

Following conclusions have been drawn from the research study conducted:

i. Discarded RO membranes were successfully converted into ultrafiltration membranes with the removal of the active polyamide layer and exposition of the polysulfone layer in experiments replicated from those contained in the published literature.

ii. Membrane conversion process was able to improve membrane permeability from 2.1 lmh/bar to over 27 lmh/bar, at least a 12 fold increase. The membranes were able to operate at a flux of between 40 – 100 lmh at a TMP of 3.5 bar, which is similar to range of flux and TMP of conventional UF membranes.

iii. Application of the converted RO membranes for ultrafiltration with LGW and CTBD feed allowed prediction of the membrane performance in terms of removal of turbidity, organics, phosphonates and improvement in SDI.

iv. Converted membrane was consistently able to reduce LGW feed water turbidity from an average value of 37 NTU to less than 1 NTU. Effluent turbidity for CTBD feed with similar feed turbidity was slightly higher (1.65 NTU), which was attributed to carryover of the chemicals used in cooling tower water treatment. COD rejection was around 70% and phosphonate rejection was around 20%. Filtrate SDI for CTBD feed was below 1.0, indicating an excellent reduction in water's fouling potential for RO membranes.

v. Membrane fouling was investigated in terms of flux decay in constant pressure mode, and correlation was explored with recognized fouling models. Membrane fouling can reasonably be explained by the different fouling models with coefficients of correlation varying from $R^2 = 0.87$ to 0.96 for the different runs and models.

vi. Higher fouling was witnessed in the LGW feed stream than in the CTBD stream despite both streams having a comparable mean turbidity. This was attributed to bigger particle size and the presence of organics in the LGW stream.

vii. Even with the incidence of fouling, the membrane can be operated at a flux range of 40 – 100 lmh, with a flux of 40 – 70 lmh used for CTBD stream with relatively stable flux throughout the filtration run.

viii. Introduction of cross-flow allowed reduction in membrane fouling. However, the cross-flow entailed limitation of the system recovery. Inhibition of flux decay was more pronounced for operation with low recoveries, which are expected to otherwise make the economics of filtration adverse.

ix. Other anti-fouling techniques were also attempted with normal backwashing sufficing for CTBD streams, and requirement of CEB/CIP for LGW stream.

5.2. Operational Guidelines for Recycled RO membranes as UF

Based on the discussion covered within this work from cited works among published literature and experimental results carried out during the course of the current research, guideline proposed for recycled RO membranes for ultrafiltration applications is tabulated in Table 12.

Table 12: Operational Guidelines for Recycled RO membranes in UF applications

Membrane Properties	
Configuration / Geometry	Spiral Wound Ultrafiltration
Membrane Active Layer	Polysulfone
Nominal Membrane Area	7.2 – 7.9 m^2 (4” element); 37.2 – 40.0 m^2 (8” element)
Membrane Dimensions	4”/8” Diameter x 40” Length (4”/8” element)
Nominal Pore Size	< 0.02 μm
Absolute Pore Size	< 0.1 μm
Application Data	
Typical Filtrate Flux Range	40 – 100 lmh
Typical Applied Feed Pressure	50 psi
Operating Mode	Dead-End or Cross-flow
Operational Cycle	Backwash-Forward Flush after 20–60 minutes
Cleaning Chemicals	NaOH + Sodium Dodecycl Sulfate NaOCl HCl
Performance Data	
Filtrate Turbidity	< 1 NTU
Filtrate SDI	< 3.0
Filtrate MFI	< 1.0
Bacteria Removal	> 3 Log

5.3. Recommendations

The following recommendations are made for continuation of research in this domain:

i. Extension of the pilot application for other similar and challenging feed streams, including:
    - Tertiary wastewater treatment for reuse
    - Secondary wastewater (as MBR)
    - Car wash water recycling

ii. Extension of pilot testing or full scale testing for long term applications, along with system automation for convenience of operation.

iii. Consideration of disinfection and sanitization measures for membrane consideration for potable water applications, especially hot water sanitization.

References

Ahmed, J., Jamal, Y., & Shujaatullah, M. (2020). Recovery of cooling tower blowdown water through reverse osmosis (RO): review of water parameters affecting membrane fouling and pretreatment schemes. *Desalination and Water Treatment, 189*, 9-17.

Ambrosi, A., & Tessaro, I. C. (2013). Study on Potassium Permanganate Chemical Treatment of Discarded Reverse Osmosis Membranes Aiming their Reuse. *Separation Science and Technology, 48*(10), 1537-1543. doi: 10.1080/01496395.2012.745876

Antony, A., Fudianto, R., Cox, S., & Leslie, G. (2010). Assessing the oxidative degradation of polyamide reverse osmosis membrane—accelerated ageing with hypochlorite exposure. *Journal of Membrane Science, 347*(1-2), 159-164.

Barassi, G., & Borrmann, T. (2012). N-chlorination and Orton rearrangement of aromatic polyamides, revisited. *Journal of Membrane Science and Technology*, *2*(2), 1000115.

BASF-Inge. (2014). inge Operator's Manual (2.1 ed.).

Bowen, W. R., & Doneva, T. A. (2000). Atomic force microscopy characterization of ultrafiltration membranes: correspondence between surface pore dimensions and molecular weight cut-off. *Surface and Interface Analysis*, *29*(8), 544-547.

Boyjoo, Y., Pareek, V. K., & Ang, M. (2013). A review of greywater characteristics and treatment processes. *Water Science and Technology*, *67*(7), 1403-1424. doi: 10.2166/wst.2013.675

Causserand, C., Rouaix, S., Lafaille, J.-P., & Aimar, P. (2008). Ageing of polysulfone membranes in contact with bleach solution: Role of radical oxidation and of some dissolved metal ions. *Chemical Engineering and Processing: Process Intensification*, *47*(1), 48-56. doi: https://doi.org/10.1016/j.cep.2007.08.013

Chesters, S. P., Pena, N., Gallego, S., Fazel, M., Armstrong, M. W., & del Vigo, F. (2013). Results from 99 seawater RO membrane autopsies. *IDA Journal of Desalination and Water Reuse, 5*(1), 40-47.

Coutinho de Paula, E., & Amaral, M. C. S. (2017). Extending the life-cycle of reverse osmosis membranes: A review. *Waste Management & Research, 35*(5), 456-470. doi: 10.1177/0734242X16684383

Coutinho de Paula, E., & Amaral, M. C. S. (2018). Environmental and economic evaluation of end-of-life reverse osmosis membranes recycling by means of chemical conversion. *Journal of Cleaner Production, 194*, 85-93.

Crittenden, J. C., Trussell, R. R., Hand, D. W., Howe, K. J., & Tchobanoglous, G. (2012). *MWH's Water Treatment: Principles and Design*: John Wiley & Sons.

D4189-07, A. (2007). Standard Test Method for Silt Density Index (SDI) of Water: ASTM International West Conshohocken, PA.

Damania, R., Desbureaux, S., Hyland, M., Islam, A., Moore, S., Rodella, A.-S., . . . Zaveri, E. (2017). *Uncharted waters: The new economics of water scarcity and variability*: The World Bank.

Darre, N. C., & Toor, G. S. (2018). Desalination of water: a review. *Current Pollution Reports, 4*(2), 104-111.

Dietz, P., Hansma, P. K., Inacker, O., Lehmann, H.-D., & Herrmann, K.-H. (1992). Surface pore structures of micro- and ultrafiltration membranes imaged with the atomic force microscope. *Journal of Membrane Science, 65*(1), 101-111. doi: https://doi.org/10.1016/0376-7388(92)87057-5

Dow-Water-and-Process-Solutions. (2011a). DOW Ultrafiltration Product Manual (3 ed.).

Dow-Water-and-Process-Solutions. (2011b). FILMTEC™ Reverse Osmosis Membranes Technical Manual. *Available on: http://msdssearch.dow.com/PublishedLiteratureDOWCOM/dh_08db/0901b803808db77d.pdf*, 609-00071.

Faigon, M. (2016). Success behind advanced SWRO desalination plant. *Filtration + Separation, 53*(3), 29-31.

Farahani, M. H. D. A., Borghei, S. M., & Vatanpour, V. (2016). Recovery of cooling tower blowdown water for reuse: The investigation of different types of pretreatment prior nanofiltration and reverse osmosis. *Journal of Water Process Engineering, 10*, 188-199.

Field, R. W., & Wu, J. J. (2011). Modelling of permeability loss in membrane filtration: Re-examination of fundamental fouling equations and their link to critical flux. *Desalination, 283*, 68-74.

Frick, J. M., Féris, L. A., & Tessaro, I. C. (2014). Evaluation of pretreatments for a blowdown stream to feed a filtration system with discarded reverse osmosis membranes. *Desalination, 341*, 126-134.

García-Pacheco, R., Javier, F., Terrero, P., Molina, S., Martínez, D., Campos, E., . . . Landaburu, J. (2016). *LIFE+ 13 TRANSFOMEM: un ejemplo de reciclaje en el mundo de la desalación*. Paper presented at the XI International Conference of Aedyr, Valencia.

García-Pacheco, R., Landaburu-Aguirre, J., Lejarazu-Larrañaga, A., Rodríguez-Sáez, L., Molina, S., Ransome, T., & García-Calvo, E. (2019). Free chlorine exposure dose (ppm· h) and its impact on RO membranes ageing and recycling potential. *Desalination, 457*, 133-143.

García-Pacheco, R., Landaburu-Aguirre, J., Molina, S., Rodríguez-Sáez, L., Teli, S. B., & García-Calvo, E. (2015). Transformation of end-of-life RO membranes into NF and UF membranes: Evaluation of membrane performance. *Journal of Membrane Science, 495*, 305-315.

García-Pacheco, R., Landaburu-Aguirre, J., Terrero-Rodríguez, P., Campos, E., Molina-Serrano, F., Rabadán, J., . . . García-Calvo, E. (2018). Validation of recycled membranes for treating brackish water at pilot scale. *Desalination, 433*, 199-208. doi: https://doi.org/10.1016/j.desal.2017.12.034

García-Pacheco, R., Lawler, W., Landaburu, J., García-Calvo, E., & Le-Clech, P. (2017). End-of-life membranes: challenges and opportunities *Chemistry, Molecular Sciences and Chemical Engineering*: Elsevier.

Gohil, J. M., & Suresh, A. K. (2017). Chlorine attack on reverse osmosis membranes: Mechanisms and mitigation strategies. *Journal of Membrane Science, 541*, 108-126.

Greenlee, L. F., Lawler, D. F., Freeman, B. D., Marrot, B., & Moulin, P. (2009). Reverse osmosis desalination: water sources, technology, and today's challenges. *Water Research, 43*(9), 2317-2348.

Guo, W., Ngo, H.-H., & Li, J. (2012). A mini-review on membrane fouling. *Bioresource Technology, 122*, 27-34.

Hermia, J. (1982). Constant pressure blocking filtration laws: application to power-law non-Newtonian fluids. *Institution of Chemical Engineers - Transactions, 60*(3), 183-187.

Hilal, N., Ogunbiyi, O. O., Miles, N. J., & Nigmatullin, R. (2005). Methods employed for control of fouling in MF and UF membranes: a comprehensive review. *Separation Science and Technology, 40*(10), 1957-2005.

Hydranautics. (2018). TSB 123.04 Disposal of Used RO Elements.

Jones, E., Qadir, M., van Vliet, M. T., Smakhtin, V., & Kang, S.-m. (2019). The state of desalination and brine production: A global outlook. *Science of the Total Environment, 657*, 1343-1356.

Kwon, Y.-N., & Leckie, J. O. (2006a). Hypochlorite degradation of crosslinked polyamide membranes: I. Changes in chemical/morphological properties. *Journal of Membrane Science, 283*(1-2), 21-26.

Kwon, Y.-N., & Leckie, J. O. (2006b). Hypochlorite degradation of crosslinked polyamide membranes: II. Changes in hydrogen bonding behavior and performance. *Journal of Membrane Science, 282*(1-2), 456-464.

Landaburu-Aguirre, J., García-Pacheco, R., Molina, S., Rodríguez-Sáez, L., Rabadán, J., & García-Calvo, E. (2016). Fouling prevention, preparing for re-use and membrane recycling. Towards circular economy in RO desalination. *Desalination, 393*, 16-30. doi: https://doi.org/10.1016/j.desal.2016.04.002

Lanxess-Lewabrane. (2012). Guidelines for the Design of Reverse Osmosis Membrane Systems. *Available on: https://lpt.lanxess.com/uploads/tx_lanxessmatrix/lew_lewabrane_manual_03_system_design_01.pdf.*

Lawler, W. (2015). Assessment of end-of-life opportunities for reverse osmosis membranes. *School of Chemical Engineering and Faculty of Engineering. Available on: http://unsworks.unsw.edu.au/fapi/datastream/unsworks:39639/SOURCE02?view=true*.

Lawler, W., Alvarez-Gaitan, J., Leslie, G., & Le-Clech, P. (2015a). Comparative life cycle assessment of end-of-life options for reverse osmosis membranes. *Desalination, 357*, 45-54.

Lawler, W., Antony, A., Cran, M., Duke, M., Leslie, G., & Le-Clech, P. (2013). Production and characterisation of UF membranes by chemical conversion of used RO membranes. *Journal of Membrane Science, 447*, 203-211.

Lawler, W., Bradford-Hartke, Z., Cran, M. J., Duke, M., Leslie, G., Ladewig, B. P., & Le-Clech, P. (2012). Towards new opportunities for reuse, recycling and disposal of used reverse osmosis membranes. *Desalination, 299*, 103-112.

Lawler, W., Leslie, G., & Le-Clech, P. (2015b). *Decision Making Tool for End-of-Life Reverse Osmosis Membrane Users*. Paper presented at the The International Desalination Association World Congress on Desalination and Water Reuse, San Diego.

Lawler, W., Wijaya, T., Antony, A., Leslie, G., & Le-Clech, P. (2011). *Reuse of reverse osmosis desalination membranes.* Paper presented at the IDA World Congress.

Li, F., Wichmann, K., & Otterpohl, R. (2009). Review of the technological approaches for grey water treatment and reuses. *Science of the Total Environment, 407*(11), 3439-3449.

Ma, J., Irfan, H. M., Wang, Y., Feng, X., & Xu, D. (2018). Recovering Wastewater in a Cooling Water System with Thermal Membrane Distillation. *Industrial & Engineering Chemistry Research, 57*(31), 10491-10499.

Martínez, S. M., Pacheco, R. G., Calvo, E. C. P., Martínez, D. Z., de la Campa, J. G., & de Abajo González, J. (2015). *Transformation of end-of-life RO membrane into recycled NF and UF membranes, surface characterization.* Paper presented at the IDA World Congress Proceeding.

Mekonnen, M. M., & Hoekstra, A. Y. (2016). Four billion people facing severe water scarcity. *Science Advances, 2*(2), e1500323.

Mohammadi, T., Kazemimoghadam, M., & Saadabadi, M. (2003). Modeling of membrane fouling and flux decline in reverse osmosis during separation of oil in water emulsions. *Desalination, 157*(1-3), 369-375.

Molina, S., Landaburu-Aguirre, J., Rodríguez-Sáez, L., García-Pacheco, R., José, G., & García-Calvo, E. (2018). Effect of sodium hypochlorite exposure on polysulfone recycled UF membranes and their surface characterization. *Polymer Degradation and Stability, 150*, 46-56.

Moradi, M. R., Pihlajamäki, A., Hesampour, M., Ahlgren, J., & Mänttäri, M. (2019). End-of-life RO membranes recycling: Reuse as NF membranes by polyelectrolyte layer-by-layer deposition. *Journal of Membrane Science, 584*, 300-308.

Morón-López, J., & Molina, S. (2020). Optimization of Recycled-Membrane Biofilm Reactor (R-MBfR) as a sustainable biological treatment for microcystins removal. *Biochemical Engineering Journal, 153*, 107422.

Morón-López, J., Nieto-Reyes, L., Aguado, S., El-Shehawy, R., & Molina, S. (2019). Recycling of end-of-life reverse osmosis membranes for membrane biofilms reactors (MBfRs). Effect of chlorination on the membrane surface and gas permeability. *Chemosphere, 231*, 103-112.

Mulder, J. (2012). *Basic principles of membrane technology*: Springer Science & Business Media.

Ould Mohamedou, E., Penate Suarez, D. B., Vince, F., Jaouen, P., & Pontie, M. (2010). New lives for old reverse osmosis (RO) membranes. *Desalination, 253*(1), 62-70. doi: https://doi.org/10.1016/j.desal.2009.11.032

Pearce, G. (2007). Introduction to membranes: Fouling control. *Filtration & Separation, 44*(6), 30-32.

Pilutti, M., Nemeth, J. E., & Nemeth, P. (2003). Technical and cost review of commercially available MF/UF membrane products. *Desalination*, 1-15.

Pontié, M. (2015). Old RO membranes: solutions for reuse. *Desalination and Water Treatment, 53*(6), 1492-1498. doi: 10.1080/19443994.2014.943060

Pontié, M., Awad, S., Tazerout, M., Chaouachi, O., & Chaouachi, B. (2017). Recycling and energy recovery solutions of end-of-life reverse osmosis (RO) membrane materials: A sustainable approach. *Desalination, 423*, 30-40. doi: https://doi.org/10.1016/j.desal.2017.09.012

Prince, C., Cran, M., LeCleche, P., Hoehn, K., & Duke, M. (2011). *Reuse and recycling of used desalination membranes*. Paper presented at the OzWater'11, Adelaide.

Qadir, M. (2020). *UN-Water Analytical Brief on Unconventional Water Resources*. Geneva, Switzerland: UN-Water.

Raval, H. D., Chauhan, V. R., Raval, A. H., & Mishra, S. (2012). Rejuvenation of discarded RO membrane for new applications. *Desalination and Water Treatment, 48*(1-3), 349-359. doi: 10.1080/19443994.2012.704727

Ren, J., Li, Z., & Wong, F.-S. (2006). A new method for the prediction of pore size distribution and MWCO of ultrafiltration membranes. *Journal of Membrane Science, 279*(1), 558-569. doi: https://doi.org/10.1016/j.memsci.2005.12.052

Revitt, D. M., Eriksson, E., & Donner, E. (2011). The implications of household greywater treatment and reuse for municipal wastewater flows and micropollutant loads. *Water Research, 45*(4), 1549-1560.

Rodríguez, J. J., Jiménez, V., Trujillo, O., & Veza, J. (2002). Reuse of reverse osmosis membranes in advanced wastewater treatment. *Desalination, 150*(3), 219-225. doi: https://doi.org/10.1016/S0011-9164(02)00977-3

Rouaix, S., Causserand, C., & Aimar, P. (2006). Experimental study of the effects of hypochlorite on polysulfone membrane properties. *Journal of Membrane Science, 277*(1), 137-147. doi: https://doi.org/10.1016/j.memsci.2005.10.040

Salahi, A., Abbasi, M., & Mohammadi, T. (2010). Permeate flux decline during UF of oily wastewater: Experimental and modeling. *Desalination, 251*(1-3), 153-160.

Saumya, S., Akansha, S., Rinaldo, J., Jayasri, M., & Suthindhiran, K. (2015). Construction and evaluation of prototype subsurface flow wetland planted with Heliconia angusta for the treatment of synthetic greywater. *Journal of Cleaner Production, 91*, 235-240.

Scott, K. (1995). *Handbook of industrial membranes*: Elsevier Science; 1st Edition.

Shi, X., Tal, G., Hankins, N. P., & Gitis, V. (2014). Fouling and cleaning of ultrafiltration membranes: A review. *Journal of Water Process Engineering, 1*, 121-138. doi: https://doi.org/10.1016/j.jwpe.2014.04.003

Shin, D. H., Kim, N., & Lee, Y. T. (2011). Modification to the polyamide TFC RO membranes for improvement of chlorine-resistance. *Journal of Membrane Science, 376*(1-2), 302-311.

Solomons, T. (1997). *Fundamentals of Organic Chemistry*. Virginia: Wiley; 5th Edition.

Terrero, P., García-Pacheco, R., Campos-Pozuelo, E., Rabadán, F., Molina-Martínez, S., de Lejarazu, A. O., & Zarzo-Martínez, D. (2017). Transformation of End-of-life RO Membrane Into Recycled NF and UF Membranes: Results of the Transformation Process and Its Validation at Pilot Scale *IDA17WC*.

Tessaro, I. C., da Silva, J. B. A., & Wada, K. (2005). Investigation of some aspects related to the degradation of polyamide membranes: aqueous chlorine oxidation catalyzed by aluminum and sodium laurel sulfate oxidation during cleaning. *Desalination, 181*(1), 275-282. doi: https://doi.org/10.1016/j.desal.2005.04.008

van Limpt, B., & van der Wal, A. (2014). Water and chemical savings in cooling towers by using membrane capacitive deionization. *Desalination, 342*, 148-155. doi: https://doi.org/10.1016/j.desal.2013.12.022

Vela, M. C. V., Blanco, S. Á., García, J. L., & Rodríguez, E. B. (2008). Analysis of membrane pore blocking models applied to the ultrafiltration of PEG. *Separation and Purification Technology, 62*(3), 489-498.

Verbeke, R., Gómez, V., & Vankelecom, I. F. (2017). Chlorine-resistance of reverse osmosis (RO) polyamide membranes. *Progress in Polymer Science, 72*, 1-15.

Veza, J. M., & Rodriguez-Gonzalez, J. J. (2003). Second use for old reverse osmosis membranes: wastewater treatment. *Desalination, 157*(1), 65-72. doi: https://doi.org/10.1016/S0011-9164(03)00384-9

Virgili, F., Pankratz, T., & Gasson, J. (2016). *IDA Desalination Yearbook 2015-2016*: Media Analytics Limited.

Wagner, T. V., Parsons, J. R., Rijnaarts, H. H. M., de Voogt, P., & Langenhoff, A. A. M. (2018). A review on the removal of conditioning chemicals from cooling tower water in constructed wetlands. *Critical Reviews in Environmental Science and Technology, 48*(19-21), 1094-1125. doi: 10.1080/10643389.2018.1512289

Zhang, X.-Q., Han, X., Zhang, X., Yang, S.-Q., & Du, M.-X. (2020). A partial feed nanofiltration system with stabilizing water quality for treating the sewage discharged from open recirculating cooling water systems. *Separation and Purification Technology, 234*, 116045.

Zhang, Y., Wang, J., Gao, F., Chen, Y., & Zhang, H. (2017). A comparison study: The different impacts of sodium hypochlorite on PVDF and PSF ultrafiltration (UF) membranes. *Water Research, 109*, 227-236. doi: https://doi.org/10.1016/j.watres.2016.11.022